67-010

UNITED STATES
NAVAL POSTGRADUATE SCHOOL

THESIS

THE BARE SURFACE EFFECT

IN CRYOGENIC PUMPING

by

Vernon Richard Everly

September 1967

THE BARE SURFACE EFFECT

IN CRYOGENIC PUMPING

by

Vernon Richard Everly
Lieutenant Commander, United States Navy
A. B., Fresno State College, 1956

Submitted in partial fulfillment of the
requirements for the degree of

MASTER OF SCIENCE IN MECHANICAL ENGINEERING

from the

NAVAL POSTGRADUATE SCHOOL
September 1967

ABSTRACT

Capture coefficients were measured for nitrogen, carbon dioxide and argon as a function of gas flow time in order to determine whether a bare surface effect existed. The effect was observed only with 300°K nitrogen on a 20°K and 24°K cryopanel and with 300°K carbon dioxide on an 82°K cryopanel. Cryopanel temperature was determined to be the only parameter influencing the bare surface effect. Capture coefficient values were representative of those reported in the literature and their dependence upon flow rate was confirmed.

TABLE OF CONTENTS

LIST OF TABLES

LIST OF ILLUSTRATIONS

LIST OF SYMBOLS

A	surface area	cm^2
A_s	cryosurface area	cm^2
f	capture coefficient	
f_g	condensation coefficient	
f_s	evaporation coefficient	
k	Boltzmann constant	erg $°K^{-1}$
M	molecular weight	gm $(gm.mole)^{-1}$
m	mass of a molecule	gm
n	number of molecules per unit volume	cm^{-3}
N	total number of molecules	
N_A	Avogadro's number	
$\dot{N}$	number of molecules per unit time	sec^{-1}
$\dot{N}_a$	summation of molecular flow into V_a	sec^{-1}
$\dot{N}_{ai}$	flow of molecules from V_a to V_i	sec^{-1}
$\dot{N}_D$	flow of molecules to diffusion pump	sec^{-1}
$\dot{N}_i$	summation of molecular flow into V_i	sec^{-1}
$\dot{N}_{io}$	flow of molecules from V_i to V_o	sec^{-1}
$\dot{N}_L$	flow of molecules into V_a from gas addition system	sec^{-1}
$\dot{N}_o$	summation of molecular flow into V_o	sec^{-1}
$\dot{N}_r$	flow of residual gas molecules	sec^{-1}
P	total pressure	torr
$\dot{P}$	pressure per unit time	torr sec^{-1}
P_e	chamber equilibrium pressure with gas flow on	torr
P_g	chamber equilibrium pressure with no gas flow	torr
P_i	pressure in V_i	torr

P_L	pressure at entrance to V_a	torr
P_o	pressure in V_o	torr
P_t	transition pressure	torr
Q_L	throughput rate	torr liter sec^{-1}
R	universal gas constant	$erg°K^{-1}gm\text{-}mole^{-1}$
S_{th}	theoretical pumping speed	liter $sec^{-1}cm^{-2}$
T	absolute temperature	°K
T_a	temperature in V_a	°K
T_g	gas temperature	°K
T_i	temperature in V_i	°K
T_L	temperature in V_L	°K
T_o	temperature in V_o	°K
T_s	temperature of the cryosurface	°K
v	velocity	cm sec^{-1}
$\bar{v}$	average molecular velocity	cm sec^{-1}
V	volume	cm^3
$\dot{V}$	volume per unit time	cm^3sec^{-1}
V_a	volume of gas addition piping	cm^3
$\dot{V}_D$	diffusion pump volumetric flow rate	cm^3sec^{-1}
V_i	volume within the radiation shielding	cm^3
V_L	volume of auxiliary vacuum system	cm^3
V_o	volume between shielding and chamber walls	cm^3
α	diffusion pump efficiency factor	
β	conductance area between V_o and V_i	cm^2
ϕ	Maxwell-Boltzmann velocity distribution function	
μ	micron	
γ	correction factor	

ACKNOWLEDGEMENTS

The work described herein was made possible by the continued support of the Office of Naval Research through the Foundation Research Program.

The author wishes to express his gratitude to Dr. Paul F. Pucci for his continued support and encouragement. He also wishes to thank Messrs. K. Smith, J. Beck, and K. Mothersell for their generous and enthusiastic assistance.

The author is deeply grateful to Mrs. Everly who typed the manuscript and continually provided encouragement and understanding during the pursuit of this work.

1. Introduction.

A bare surface phenomenon in cryopumping experiments has been reported by several investigators, (1,6,17,20), while one investigator (5) reported that no such phenomenon occurred under equivalent conditions. This is a transient condition that takes place when a clean cryosurface is initially cryogenically cooled. As time increases, the pumping rate increases noticeably, then steadies to a constant rate. It is the purpose of this work to ascertain the existance of the bare surface effect, at least for three common gases: nitrogen, carbon dioxide and argon. In order to achieve these results, the capture coefficients of these gases must be determined as a function of time. Hence, as a secondary purpose, the values of the capture coefficients may be compared with those presently published in the literature.

2. Cryogenic Pumping.

With the advent of the space age, the need for ultrahigh vacuum systems has arisen in order that simulation of the conditions to be met by vehicles in outer space may be achieved. When the extremely high cost of accomplishing a space mission and the tremendous complexity of the equipment carried are considered, it becomes very evident that preliminary research under conditions encountered in the space environment are necessary. In order to simulate the outer space environment in the laboratory, ultrahigh vacuums of the order 10^{-8} torr to 10^{-13} torr are required.

Among the important parameters necessary to design an ultrahigh vacuum system are the expected gas load and the operating pressure. Space simulation systems require extremely large volumes and generate appreciable gas loads, thus requiring systems capable of high pumping speeds and low pressures. The use of mechanical and diffusion pumps alone becomes prohibitively expensive due to the large sizes required to achieve high pumping speeds.

Cryogenic pumping, referred to in the literature as cryopumping, is a process where gas in a vacuum chamber is subjected to a surface cold enough to freeze gas molecules on contact. As sufficient gas molecules are trapped, the pressure of the system is decreased. The gases condense as long as their partial pressures are higher than the equilibrium vapor pressure at the temperature of the condensing surface. Liquified gases, such as helium, nitrogen and hydrogen provide a convenient means of obtaining the cold surface required. Helium has been used by most investigators due to the relative safety involved, and the fact that it will cryopump all other gases.

In order to predict the ability of a cold surface to condense gases, a dimensionless parameter known as the capture coefficient has been introduced, which is generally defined as the probability that a gas molecule will condense on a cold surface in its first collision with that surface. The only analytical work done in the area of solid-gas interface reactions has been by Lennard-Jones in 1936, by the methods of quantum mechanics (15). However, due to the difficulties involved in solving the equations, there still remains a lack of understanding of the solid-gas interface phenomenon. Therefore, the requirement for the surface area of a cryopump in an engineering application cannot be ascertained unless the capture coefficient of that gas has already been experimentally determined.

In order to recognize the advantages and limitations of cryopumping, Figure 1 has been included. The vapor pressure of a solified gas, as a function of absolute temperature, may be described by

$$\log_{10} P = A - B/T \qquad (2.1)$$

where A and B are constants, and T is the Kelvin temperature (2). With a gaseous helium refrigerator, the cryopanel can be maintained at approximately 20°K or slightly lower. Therefore neon, hydrogen, and helium (not included in Figure 1) could not be pumped and are generally referred to as noncondensables. Since these three gases usually represent only a small fraction of the total load in an engineering application, the 20°K temperature has been accepted as a practical operating point. However, if these noncondensables must be pumped, it has been found more advantageous to augment the vacuum system with an auxiliary cryosorption array (11). Another limitation of the cryopump is the buildup of condensate on the cold surface. As this layer increases in thickness, the temperature

at the outer surface increases thus increasing the number of noncondensable gases in the system.

These limitations may be effectively reduced by utilizing a mechanical pump and oil diffusion pump to increase the vacuum as much as possible prior to cooling the cryopump. This allows a much smaller buildup of condensate to take place and decreases the number of warmup periods required. In addition, the diffusion pump will reduce the partial pressures of noncondensable gases.

3. Theoretical Development of the Capture Coefficient.

Although various investigators have defined the capture coefficient in a number of ways, the simplest to develop in terms of experimental parameters is that of Dawson and Haygood (9). The treatment in this work is general and follows closely that of the above investigators.

The capture coefficient is defined as the ratio of the actual number of molecules captured by a cold surface to the theoretical maximum number of molecules which could be captured. The actual number of molecules captured by the cryosurface is thus defined as the experimental pumping speed, $\dot{V}_{exp}$, and the theoretical maximum number of molecules which may be captured is defined as the theoretical pumping speed, $\dot{V}_{th}$. Therefore the capture coefficient is

$$f = \frac{\dot{V}_{EXP}}{\dot{V}_{TH}} \tag{3.1}$$

As the pressure decreases in a vacuum system, the frequency of intermolecular collisions decreases to a very low rate and results in a long mean free path. Therefore molecular collisions with the chamber walls occur more frequently. This general area is known as the free molecular region as contrasted to the continuum region at atmospheric pressure. In the free molecular region, condensation and evaporation phenomenon may be derived mathematically through the use of kinetic theory to advantage. Since several basic concepts will be utilized later, they are presented here for reference.

a. Average Molecular Velocity.

The Maxwell-Boltzmann velocity distribution function is defined as the fractional number of molecules in the velocity range from v to v + dv per unit of velocity range and is

$$\phi = \frac{4}{\pi}\left[\frac{m}{2kT}\right]^{3/2} v^2 \quad EXP\left[-\frac{mv^2}{2kT}\right] \tag{3.2}$$

Then the average velocity is

$$\bar{V} = \frac{\int_0^\infty v\,\phi\,dv}{\int_0^\infty \phi\,dv} = \left[\frac{8kT}{\pi m}\right]^{1/2} \tag{3.3}$$

where k = Boltzmann constant, ergs/°K.

T = absolute temperature, °K.

m = mass of one molecule, grams.

b. Pressure.

The pressure within a chamber is

$$P = \frac{1}{3} n m \bar{v}^2 = n k T \tag{3.4}$$

where n = number of molecules per unit volume, cm^{-3}.

c. Ideal Gas Law.

The ideal gas law may be derived directly from (3.4) and expressed as

$$PV = NkT \tag{3.5}$$

where V = volume, cm^{-3}

N = total number of molecules.

d. Number of Molecules Incident on a Surface.

The number of molecules incident on a surface per unit time is

$$\dot{N} = \frac{1}{4} A n \bar{v} \tag{3.6}$$

where $\dot{N}$ = number of molecules per unit time, sec^{-1}

A = surface area, cm^2

Substitution of (3.3) and (3.4) into (3.6) yields

$$\dot{N} = \frac{PA}{(2\pi m k T)^{1/2}} \tag{3.7}$$

e. Thermal Transpiration.

The interrelationship between pressure and temperature of a particular gas system in the free molecular region is called thermal transpiration and is given by (12) as

$$\frac{P}{\sqrt{T}} = \text{constant}$$

For example, when two volumes are separated by a flow conductance, such as an aperature, the thermal transpiration effect is given by

$$\frac{P_1}{\sqrt{T_1}} = \frac{P_2}{\sqrt{T_2}} \tag{3.8}$$

This relationship is also applicable to pressure gages when they are used at a temperature different from the calibration temperature.

f. Theoretical Pumping Speed.

The theoretical pumping speed was defined as the maximum number of molecules which may be captured by the cold surface per unit time. If every molecule that strikes the surface sticks, then the theoretical specific pumping speed is given by

$$S_{TH} = \frac{\dot{V}}{A} \tag{3.9}$$

where $\dot{V}$ = volume per unit time, $cm^3\ sec^{-1}$.

Solving (3.5) for V and taking the time derivative yields

$$\dot{V} = \frac{\dot{N} k T}{P} \tag{3.10}$$

and substitution into (3.9) gives

$$S_{TH} = \left[\frac{kT}{2\pi m}\right]^{1/2} \tag{3.11}$$

Since $k = R/N_A$ and $m = M/N_A$

where R = universal gas constant, erg/gm-mole°K

N_A = Avogadro's number, $(\text{gm-mole})^{-1}$

M = molecular weight, gm/gm-mole,

the theoretical specific pumping speed may be expressed as

$$S_{TH} = \left[\frac{RT}{2\pi M}\right]^{1/2} \tag{3.12}$$

The theoretical volumetric pumping speed from (3.9) is

$$\dot{V}_{TH} = A_s \left[\frac{RT_g}{2\pi M}\right]^{1/2} \tag{3.13}$$

where the subscript "g" refers to the gas and "s" to the cryosurface.

g. Experimental Pumping Speed.

The experimental pumping speed may be developed by utilizing the continuity condition on a system to which a gas load has been applied. Then

$$\frac{P_L \dot{V}_L}{RT_L} = \frac{P\dot{V}}{RT_g} + \frac{\dot{P}V}{RT_g} \tag{3.14}$$

where the subscript "L" refers to conditions at the controlled leak. The left-hand side of the equation represents the rate of flow of gas into the system and the right-hand side the total number of moles of gas condensed per second. If an equilibrium pressure P_e is reached in the system, $\dot{P}$ is zero and

$$\frac{P_L \dot{V}_L}{RT_L} = \frac{P_e \dot{V}}{RT_g} \tag{3.15}$$

The gas throughput rate Q_L may be defined as

$$Q_L = P_L \dot{V}_L \tag{3.16}$$

exists between the gas and solid phases. This is the situation in the experimental apparatus.

The rate of condensation of the gas is

$$\dot{N}_{COND} = \frac{f_g P_g A_s}{(2\pi m k T_g)^{1/2}} \tag{3.21}$$

and the rate of evaporation of the solid phase is

$$\dot{N}_{EVAP} = \frac{f_s P_s A_s}{(2\pi m k T_s)^{1/2}} \tag{3.22}$$

where the subscript "g" refers to the gas and "s" to the condensate surface. The parameters f_g and f_s are the condensation and evaporation coefficients respectively, and are defined as the ratio of actual molecular flux to the theoretical molecular flux. Hence f_g is essentially a cryopumping efficiency. Again, at the equilibrium condition, the condensation and evaporation rates are equal and the relationship between phases is

$$\frac{f_g P_g}{\sqrt{T_g}} = \frac{f_s P_s}{\sqrt{T_s}} \tag{3.23}$$

Note that there will be a net transfer of energy but no mass transfer.

When a transient system is considered, where a stream of gas is admitted to the system while the cryosurface is simultaneously pumping, equilibrium may again be achieved at some chamber pressure P_e. The actual capture rate of molecules on the cold surface is the difference between the condensation and evaporation rates

$$\dot{N}_{ACT} = \frac{f_g P_e A_s}{(2\pi m k T_g)^{1/2}} - \frac{f_s P_s A_s}{(2\pi m k T_s)^{1/2}} \tag{3.24}$$

where P_e is the equilibrium chamber pressure with the gas flow on and P_s is the vapor pressure of the solid phase. The theoretical incidence rate of molecules on the cold surface is given by (3.7) as

$$\dot{N}_{TH} = \frac{P_e A_s}{(2\pi m k T_g)^{1/2}} \tag{3.25}$$

The ratio of $\dot{N}_{act}$ to $\dot{N}_{th}$ by definition is the capture coefficient and yields

$$f = f_g \left[1 - \frac{f_s P_s \sqrt{T_g}}{f_g P_e \sqrt{T_s}} \right] \tag{3.26}$$

From (3.23)

$$f_s = f_g \frac{P_g \sqrt{T_s}}{P_s \sqrt{T_g}} \tag{3.27}$$

Substitution of (3.27) into (3.26) gives

$$f = f_g \left[1 - \frac{P_g}{P_e} \right] \tag{3.28}$$

where P_g is the pressure in the chamber with no gas flow and P_e is the equilibrium pressure with flow. Equation (3.28) is the desired relationship between the capture and condensation coefficients.

4. Experimental Determination of the Bare Surface Effect.

4.1 Experimental Technique.

To determine the existence of a bare surface effect, the capture coefficient must be determined as a function of time. Hence the basic consideration is to calculate a capture coefficient sequentially for a large number of runs while allowing the condensate to build up. One investigator reported the duration of the effect to be about 25 minutes (20). In order to determine whether other parameters may influence the bare surface effect, the flow rate, cryosurface temperature and gas temperature must be varied.

A schematic of the experimental system is shown in Figure 2, and a detailed description is contained in Appendix A. The system consists of a vacuum chamber with a cylindrical center section shield and two disc end shields. The cryopanel is suspended from the top of the chamber and has fill and vent lines to the outside. A high vacuum gate valve separates the chamber from the diffusion pump and the latter is backed by a large mechanical forepump. The test gas is introduced through the front shield and the line has an optical baffle installed to prevent streaming. For convenience all valves are air operated and arranged with the instrumentation at a console.

Figure 3 is an example of a plot of pressure versus time that would be obtained during an experimental run if only condensable gases were present. At time t_1, the controlled leak is open to the chamber and the system is at equilibrium with the diffusion pump and cryosurface pumping. At time t_2, the chamber is isolated from the diffusion pump by an air operated gate valve. With the same in-flow of gas, a surge takes place until the cryopump can restore equilibrium at some pressure P_e. At time t_3, the controlled leak is secured by an air operated gate valve and a

pressure drop occurs. A new equilibrium pressure P_g will be reached with no gas flow into the chamber. Measurement of $\Delta P = P_e - P_g$ is critical and will be developed in section 4.3.

The above technique will determine the capture coefficient of the gas under investigation. By recording the time at the measurement of ΔP and making a sequence of runs, a plot of capture coefficient versus time can be constructed.

The experiments were designed to examine nitrogen, carbon dioxide, and argon, since the bare surface effect was observed with these gases. Also capture coefficient data was available for comparison as a secondary objective. Since Bevan's work (3) with nitrogen showed the dependence of capture coefficients on flow rate, it was decided to examine the three gases at two flow rates which had magnitudes significantly different, and would be comparable to the few flow rates reported in the literature. The values chosen were 0.2 torr liter/sec and 3×10^{-3} torr liter/sec. In order to determine more criteria for the bare surface effect, it was decided to make several runs with carbon dioxide at a liquid nitrogen panel temperature of 77°K. Argon was not considered since its fusion temperature of 84°K was so close to liquid nitrogen temperature. Any small increase in the panel temperature would cause the condensed argon to evaporate and pressure bursts would occur in the system rendering the recording equipment useless.

Before each experiment, the system was allowed to pump to a base pressure which generally was 5×10^{-7} torr with the cryopanel at room temperature. Upon cooling the cryopanel, the pressure was reduced to 2×10^{-8} torr, hence a minute amount of condensate was present at the start of each experiment. It is considered that this extremely small amount of condensate had negligible effect on the results of the

experiments.

In order that conditions would be the same for every determination of the capture coefficient in each experiment a routine was established. Prior to each determination, the ionization gage was degassed for a period of 45 seconds, then zeroed and checked at full scale for ion current. This insured a calibrated gage at all times. During each determination, the 19 thermocouples were recorded on the printer to insure constant temperatures at the cryopanel and to observe the gas temperature at the shields. The ideal situation for the experiments would have been to obtain instantaneous capture coefficients with a continuous gas flow. However, since the method of measuring ΔP requires stopping the gas flow, this could not be done. Hence the actual time for each experiment was approximately two hours while the actual gas flow time was of the order of 25 to 45 minutes. In each case data was taken until all transients had subsided. These values were then reported as the capture coefficient. Calculation of the capture coefficients was done by the method presented in Appendix F.

Other methods of measuring the gas flow time were considered. A good method would have been to start with a bare surface and allow gas to flow until some time, t_1, then stop and warm up the panel. Beginning again with a bare surface, start the gas flow and continue to time t_2, where $t_2 > t_1$. Continuing this process until the transients had subsided would have produced the same curves as this work. This method was not selected since nearly 24 hours are required to warm up the panel prior to each experiment to insure a bare surface.

4.2 Experimental Equations.

When equation (3.18) is substituted into (3.28) and solved for the condensation coefficient, the following expression is obtained:

$$f_g = \frac{Q_L T_g}{\Delta P A_s T_L} \left[\frac{2\pi M}{R T_g} \right]^{1/2} \qquad (4.1)$$

The capture coefficient may be calculated from equation (3.28) and is repeated here for clarity.

$$f = f_g \left[1 - \frac{P_g}{P_e} \right] \qquad (3.28)$$

If $P_e \gg P_g$, then the condensation coefficient is equal to the capture coefficient.

Corrections must be applied to equation (4.1) due to design considerations of the experimental apparatus. Ionization gages are calibrated with nitrogen at ambient room temperature. Therefore a gage factor must be applied for each gas tested other than nitrogen. Since

$$\Delta P_{ACT} = (G.F.)\, \Delta P_m$$

where G.F. is the gage factor and the subscript "m" refers to the measured pressure drop, then equation (4.1) becomes

$$f_g = \frac{Q_L T_g}{A_s T_L \Delta P (G.F.)} \left[\frac{2\pi M}{R T_g} \right]^{1/2} \qquad (4.2)$$

The thermal transpiration equation (3.8) must also be applied if the calibration temperature is different from the temperature at the gage site. During the experimental work, the nude gage in the inner volume was inoperative and the ionization gage mounted in the wall of the outer volume was used for all pressure measurements. Hence no thermal transpiration correction was required. However since the outer gage was used, the conductance effect must be considered. The equation for the relationship

between capture coefficient and conductance area is derived in Appendix E and is repeated here for clarity.

$$\frac{f^*}{f} = \frac{\mathcal{B} - f^* A}{\mathcal{B}} \qquad \text{(E.41)}$$

where $\mathcal{B}$ = conductance area

f* = capture coefficient measured without conductance

f = capture coefficient measured with conductance

Then

$$f^* = \frac{1}{\frac{1}{f} + \frac{A}{\mathcal{B}}} \qquad (4.3)$$

Since the partial pressure of the test gas could not be measured, condensation coefficients rather than capture coefficients were measured. Hence in equation (4.3) the subscript "g" may be added and

$$f_g^* = \frac{1}{\frac{1}{f_g} + \frac{A}{\mathcal{B}}} \qquad (4.4)$$

where f_g is calculated from equation (4.2). A digital computer program was written to perform the calculations and is included as Appendix G.

4.3 Experimental Measurements.

The parameters in equation (4.2) that must be measured in order to calculate the condensation coefficient are: (a) the pressure drop, ΔP; (b) the gas temperature in the chamber, T_g, and the temperature at the controlled leak, T_L; and (c) the throughput at the controlled leak, Q_L. The remaining parameters are constants of the system or the gas under investigation.

(a) Pressure Drop Measurement.

The pressure drop is essentially the most critical measurement made in order to calculate the capture coefficient. A rigorous treatment is included in Appendix E.

The experimental equipment has two Bayard-Alpert ionization gages installed, one nude within the radiation shielding, the other a conventional glass envelope type mounted on the wall of the chamber. A cold cathode trigger gage is also mounted on the chamber wall. With these gages only the total chamber pressure may be measured, which is the sum of the partial pressures of all the gases present. In the previous analysis an assumption was made that only a pure condensable gas was leaked into the system, and no consideration was given to inleakage through the system walls and seals nor to out-gassing from system components on the vacuum side. Hence other condensables and noncondensables will be present in variable amounts, and the resulting pressure versus time curve is shown in Figure 4. The partial pressure of the test gas can be measured with a mass spectrometer, but this equipment was not available.

In order to reduce the effects of other condensable and noncondensable gases, only high purity special research gases were used. The assumption must therefore be made that all other gases are present in negligible quantities as compared to the test gas.

(b) Gas Temperature.

In section 3, the derivations were based on the fundamental Maxwell-Boltzmann velocity distribution. In order that this approach be valid, the ratio of radiation shield wall surface to cryosurface must be large so that the gas molecules will collide with the walls prior to striking the cryopanel. Also the wall temperature must be maintained constant and uniform. If these conditions are satisfied, the gas temperature T_g will be that of the radiation shields. Thermocouples were installed on the cryopanel, radiation shields and variable leak line to record temperatures and are shown in Figure 5. An automatic digital voltmeter - printer unit was used to monitor temperatures continually to

insure validity.

(c) Throughput at the Controlled Leak.

The flow rate was calculated by measuring the rate of pressure rise in a known volume. A schematic is shown in Figure 6, and the experimental procedure is discussed in detail in Appendix C.

5. Discussion of Results

5.1 Experimental Results

Figures 7 through 13 are the results of the experiments to determine the bare surface effect. Data for the curves are presented in Tables I through VII. Most of the experimental work was done for a gas temperature of 300°K and a cryopanel temperature of 19°K to 25°K. Only one successful experiment was made at a panel temperature of 82°K and is shown in Figure 13 for carbon dioxide. Trouble was experienced with inleakage around the o-rings when liquid nitrogen was used in the cryopanel.

The results of the experiments at a 300°K gas temperature and 19°K to 25°K cryopanel temperature are as follows:

(a) Nitrogen.

The bare surface effect was observed as shown in Figures 7 and 8 for both high and low flow rates. At the high flow rate the transient occurred for only eight minutes, while at the low flow rate, an initial transient occurred for four minutes, then took about 40 minutes at a constant positive slope to reach the steady state. Hence it may be important in specific applications to allow for the transient time before full pumping speed is available. Full pumping speed would be available within eight minutes if nitrogen were the principle constituent to be pumped at high flow rates.

(b) Carbon Dioxide.

The bare surface effect was not observed as shown in Figures 9 and 10 for either flow rate. The experimental points had a minimum of scatter and were essentially flat. Full pumping speed is available immediately if carbon dioxide is the principle constituent to be pumped.

(c) Argon.

The bare surface effect was not observed as shown in Figures 11 and 12 for either flow rate. At the higher flow rate very little scatter was observed in the experimental points, while at the lower flow rate extreme scatter was observed for the first 70 minutes. However the next 57 minutes showed little scatter and the curve was essentially flat. Again full pumping speed is available immediately if argon is the principle constituent to be pumped.

The results of the carbon dioxide experiment at a 300°K gas temperature and 82°K cryopanel is shown in Figure 13. The bare surface effect was observed and the transient period was about seven minutes.

Capture coefficients at the steady state for various flow rates are presented in Tables VIII, IX and X. Values are representative of those found by other investigators and a comparison will be made in section 5.2.

One other possibility is apparent from the design of the system that would preclude a bare surface prior to condensing a gas on the cryopanel. Oil from either the diffusion pump or introduced with impure test gas may deposit on the panel. All precautions were taken in these experiments to exclude this possibility. Only high purity test gas was used and the liquid nitrogen trap above the diffusion pump was filled at all times. Also it has been observed that oil deposits on a cryopanel will become visible and appear as a spectrum of light as the condensed gas begins to change state upon warming the panel. Observations were made after every experiment and no oil deposit effects were seen.

It was also interesting to note that on warm up of the cryopanel the visible condensed gases behaved differently. Argon tended

to ripple and flake off in about one inch pieces. Nitrogen appeared to become wet and slide off the panel to the bottom of the vacuum tank in large pieces. Carbon dioxide sublimed at 194°K.

5.2 Comparison with Published Data.

The bare surface effect was first reported by Wang, Collins and Haygood in 1962. Since that time various investigators have reported the phenomenon for different gases at generally different conditions. One group of investigators reported that the effect did not exist and others, recognizing that the effect may exist, condensed the test gas on the cryopanel until a coating was visible, prior to measuring the capture coefficient. Table XI is a compilation of all known references to the bare surface effect. All investigators observed the bare surface effect unless otherwise specified.

For carbon dioxide at a gas temperature of 300°K and a 77°K cryopanel temperature, all investigators with the exception of reference (5) observed the bare surface effect. Since flow rates were widely varied, it is considered that throughput is not a parameter. When the panel temperature was reduced to about 20°K the bare surface effect was not observed. Hence it is considered that the panel temperature is a parameter influencing the bare surface effect.

Both argon and nitrogen confirm the above conclusion that throughput is not a parameter. Argon did not show a bare surface effect while nitrogen did. However the literature does show that for nitrogen at a gas temperature of 79°K and an 18°K panel temperature the bare surface effect was not observed, hence it may be considered that the gas temperature is not a parameter influencing the phenomenon. The bare surface effect was also observed in hydrogen but no other experimental evidence

is available for comparison.

It is difficult to compare capture coefficients since many investigators have not published enough basic data. In most cases, flow rates are deleted, and cryopanel temperatures are usually listed at the temperature of the cryofluid used for cooling, not the actual surface temperature which may be greatly different. Also it was noted that in some cases the capture coefficient value was arrived at by averaging many experimental runs, when in reality conditions were different for each run. Hence any comparison of published results must be done with care. Therefore the values in Tables VIII, IX, and X are for specific flow rates and at the steady state condition, after all transient effects have died away in the cases where they were observed.

It may be observed from the tables that the capture coefficients of the gases investigated are functions of flow rate, gas temperature and cryopanel temperature. Enough data had not appeared in the literature previously to see the effect of flow rate on capture coefficients. Bevan (3) showed that nitrogen capture coefficients were dependent on flow rate and the values from Table VIII confirm his work. The values from Table IX for 300°K carbon dioxide at a 77°K panel temperature have been plotted in Figure 14 and also confirm the dependence of the capture coefficients for this gas on flow rate. It is significant that the values agree so well from three different investigators. The values from Table X for this work show that the capture coefficients of argon are dependent on flow rate. Hence it would be expected that all gases should exhibit this characteristic and all capture coefficient values reported in the literature must be accompanied by flow rate values in order to have meaning.

6. Uncertainty Analysis.

Since the condensation coefficient was calculated in this work in order to detect the bare surface effect, an analysis must be made to judge the reliability of the results. The method of Kline and McClintock (13) was used in that all variables were assumed to have a normal or Gaussian distribution and the condensation coefficient was essentially a linear function of several independent variables. Then

$$\left[\frac{\Delta f_g}{f_g}\right]^2 = \left[\frac{\Delta x_1}{x_1}\right]^2 + \left[\frac{\Delta x_2}{x_2}\right]^2 + \cdots + \left[\frac{\Delta x_n}{x_n}\right]^2 \qquad (6.1)$$

where the x's are variables.

From equation (4.2) with some rearrangement,

$$f_g = \text{CONSTANT} \cdot \frac{\dot{P}_L V_L T_g^{1/2}}{A_s T_L \Delta P} \qquad (6.2)$$

Hence six independent variables must be considered. Additionally the variable β must be included from equation (4.4) for conductance effects. When substituted into equation (6.1) it is seen that,

$$\left[\frac{\Delta f_g}{f_g}\right]^2 = \left[\frac{\Delta \dot{P}}{\dot{P}}\right]^2 + \left[\frac{\Delta V_L}{V_L}\right]^2 + \frac{1}{4}\left[\frac{\Delta T_g}{T_g}\right]^2 + \qquad (6.3)$$

$$\left[\frac{\Delta A_s}{A_s}\right]^2 + \left[\frac{\Delta T_L}{T_L}\right]^2 + \left[\frac{\Delta(\Delta P)}{(\Delta P)}\right]^2 + \left[\frac{\Delta \beta}{\beta}\right]^2$$

The accepted values of the variables, their uncertainties and the $\frac{\Delta x}{x}$ are listed in Table XII. V_L, A_S and β are all averages of several measurements and the uncertainties were judged from differences in measurements. The thermocouples were calibrated with ice and liquid

nitgrogen junctions and the values substituted into a National Bureau of Standards computer program (16). Voltages were reproducible within ten microvolts at 20°K which gave an accuracy of about 2°K. The pressure drop was measured with an ionization gage which has a 2% accuracy as stated by the manufacturer. $\dot{P}_L$, the pressure rise used to measure the flow rate, was measured with a thermocouple gage. The average difference found in the measurements was two parts in 21 yielding a fraction of 0.095.

Substituting the values of $\frac{\Delta x}{x}$ from Table XII into equation (6.3) and taking the square root yields

$$\frac{\Delta f_g}{f_g} = 0.118 \qquad (6.4)$$

7. Conclusions.

The bare surface effect was observed with 300°K nitrogen on a 20°K to 24°K cryopanel. The effect was not observed at the same conditions with argon or carbon dioxide. The effect was observed with 300°K carbon dioxide on an 82°K cryopanel. It is concluded that flow rate and gas temperature are not parameters influencing the bare surface effect, but the cryopanel temperature is a factor.

Capture coefficients are dependent upon flow rate, gas temperature and cryopanel temperature. Up to this time flow rate has not been recognized as an influence. Therefore published capture coefficients have little value unless accompanied with flow rate data. Capture coefficients show significant differences in value from high to low flow rates.

The theoretical understanding of solid-gas interfaces has not progressed since the work of Lennard-Jones and Devonshire (15) in 1936 and probably will not with present day knowledge of quantum mechanics. Therefore to utilize our present design concepts, more empirical relations must be developed from experimental data. It is hoped that the results of this work will provide other investigators with a part of the necessary knowledge to do so.

BIBLIOGRAPHY

1. Albero, C. M., "Design and Development of a Cryogenic Pumping Evaluation Facility", M. S. Thesis, Naval Postgraduate School, 1965.

2. Bailey, B. M., and Chuan, R. L., "Cryopumping for High Vacuum with Low Power", 1958 Vacuum Symposium Transactions, 262, Pergamon Press, Inc., 1959.

3. Bevan, J. A., "Capture Coefficients of Nitrogen on a Cryogenically Cooled Panel", M. S. Thesis, Naval Postgraduate School, 1967.

4. Brown, R. F., and Wang, E. S. J., "Capture Coefficients of Gases at 77°K", Advances in Cryogenic Engineering, Vol. 10, Plenum Press, 1965.

5. Buffham, B. A., Henault, P. B., and Flinn, R. A., "A Theoretical Evaluation of the Sticking Coefficient in Cryopumping", 1962 Vacuum Symposium Transactions, 205, Pergamon Press, Inc., 1963.

6. Chubb, J. N., Gowland, L., and Pollard, I. E., "Condensation Pumping of Hydrogen and Deuterium on Liquid Helium Cooled Surfaces", 1966 Vacuum Symposium Abstracts, Herbick and Held Printing Co., Pittsburg, Penna., 1966.

7. Dawson, J. P., Haygood, J. D., and Collins, J. A., Jr., "Temperature Effects on the Capture Coefficients of CO_2, N_2, and A", Advances in Cryogenic Engineering, Vol. 9, Plenum Press, Inc., 1963.

8. Dawson, J. P., "Capture Coefficients of Six Common Gases", Technical Report, AEDC-TDR-64-84, May, 1964.

9. Dawson, J. P., and Haygood, J. D., "Cryopumping", Cryogenics, Vol. 5, April, 1965.

10. Dayton, B. B., "Outgassing Rate of Contaminated Metal Surfaces", 1961 Vacuum Symposium Transactions, Pergamon Press, Inc., 1962.

11. John, J. E. A., and Hardgrove, W. F., "Development of a Test Plan for Evaluation of a Cryosorption Vacuum System", Technical Report, GSFC 332-Y-09-04, January, 1965.

12. Kennard, E. H., Kinetic Theory of Gases, McGraw Hill Inc., 1938.

13. Kline, S. J., and McClintock, F. A., "Uncertainties in Single-Sample Experiments", Mechanical Engineering, January, 1953.

14. LaChance, G. M., "The Theory and Construction of a Liquid Helium Cryopump", M. S. Thesis, Naval Postgraduate School, 1964.

15. Lennard-Jones, J. E., and Devonshire, A. F., "The Interaction of Atoms and Molecules with Solid Surfaces. IV-The Condensation and Evaporation of Atoms and Molecules", Proc. Roy. Soc. (London), Ser. A156, No. A, 887, 6 August 1936.

16. Powell, R. L., and Sparks, L. L., "Available Low Temperature Thermocouple Information and Service", NBS Report 8750, February, 1965.

17. Rogers, K. W., "Experimental Investigations of Solid Nitrogen Formed by Cryopumping", NASA CR-553, August, 1966.

18. Tedeschi, L. C., "Capture Coefficients of Carbon Dioxide and Nitrogen Gas on a Cryogenic Cooled Surface", M. S. Thesis, Naval Postgraduate School, 1966.

19. Van Atta, C. M., Vacuum Science and Engineering, McGraw Hill Inc., 1965.

20. Wang, E. S. J., Collins, J. A. Jr., and Haygood, J. D., "General Cryopumping Study", Advances in Cryogenic Engineering, Vol. 7, Plenum Press, 1962.

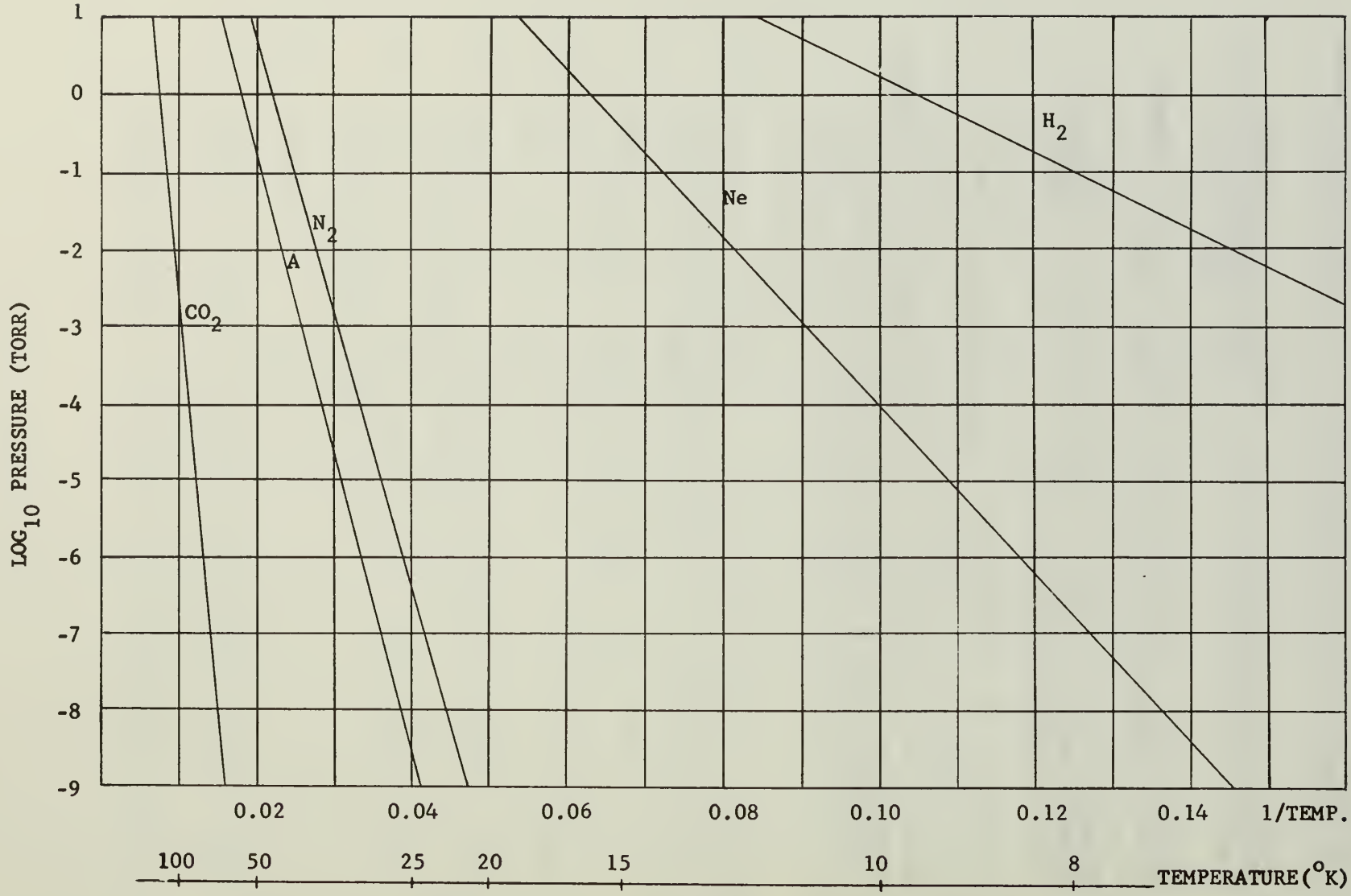

FIGURE 1. VAPOR PRESSURE OF VARIOUS GASES

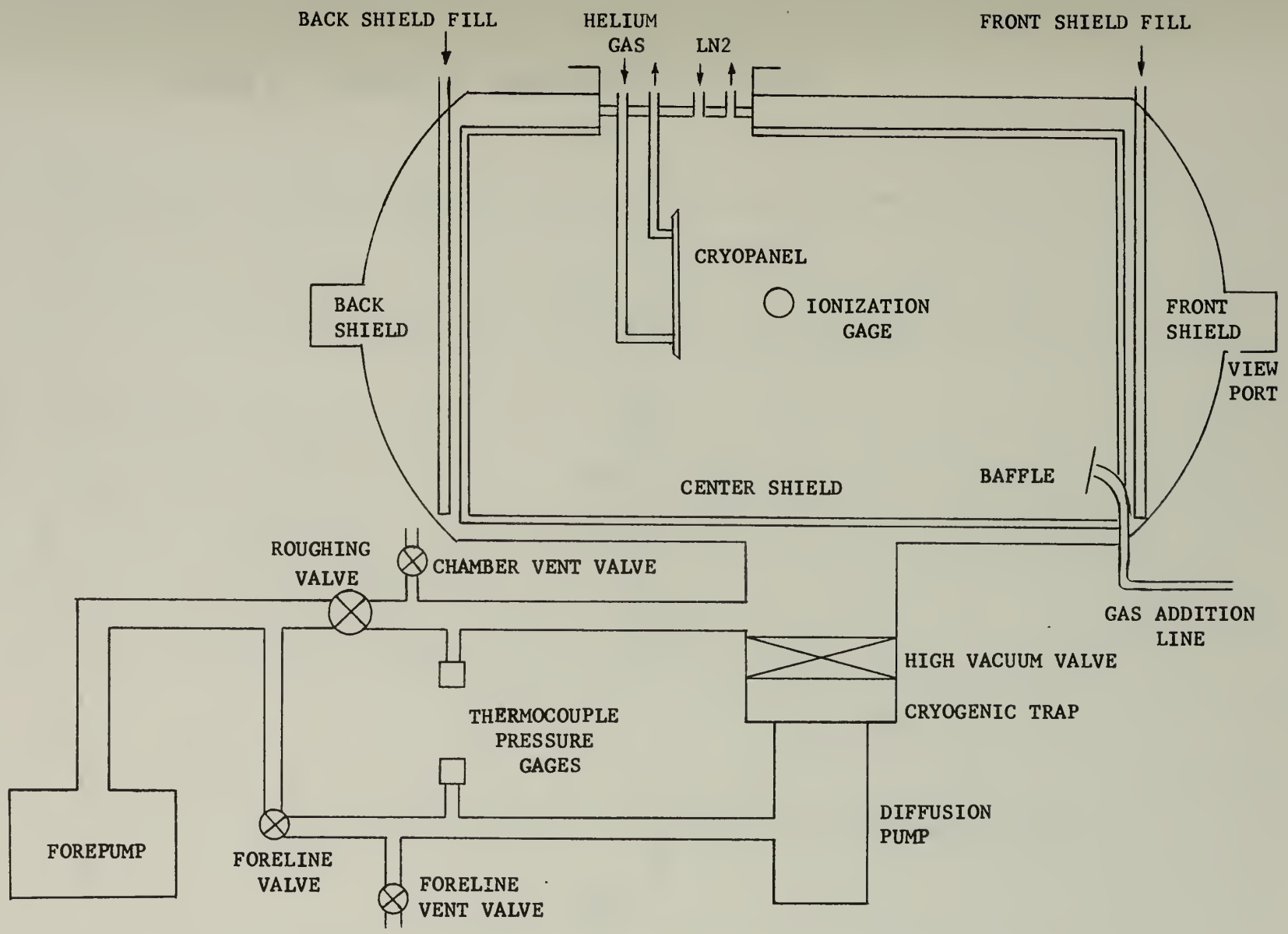

FIGURE 2. SCHEMATIC OF THE SYSTEM

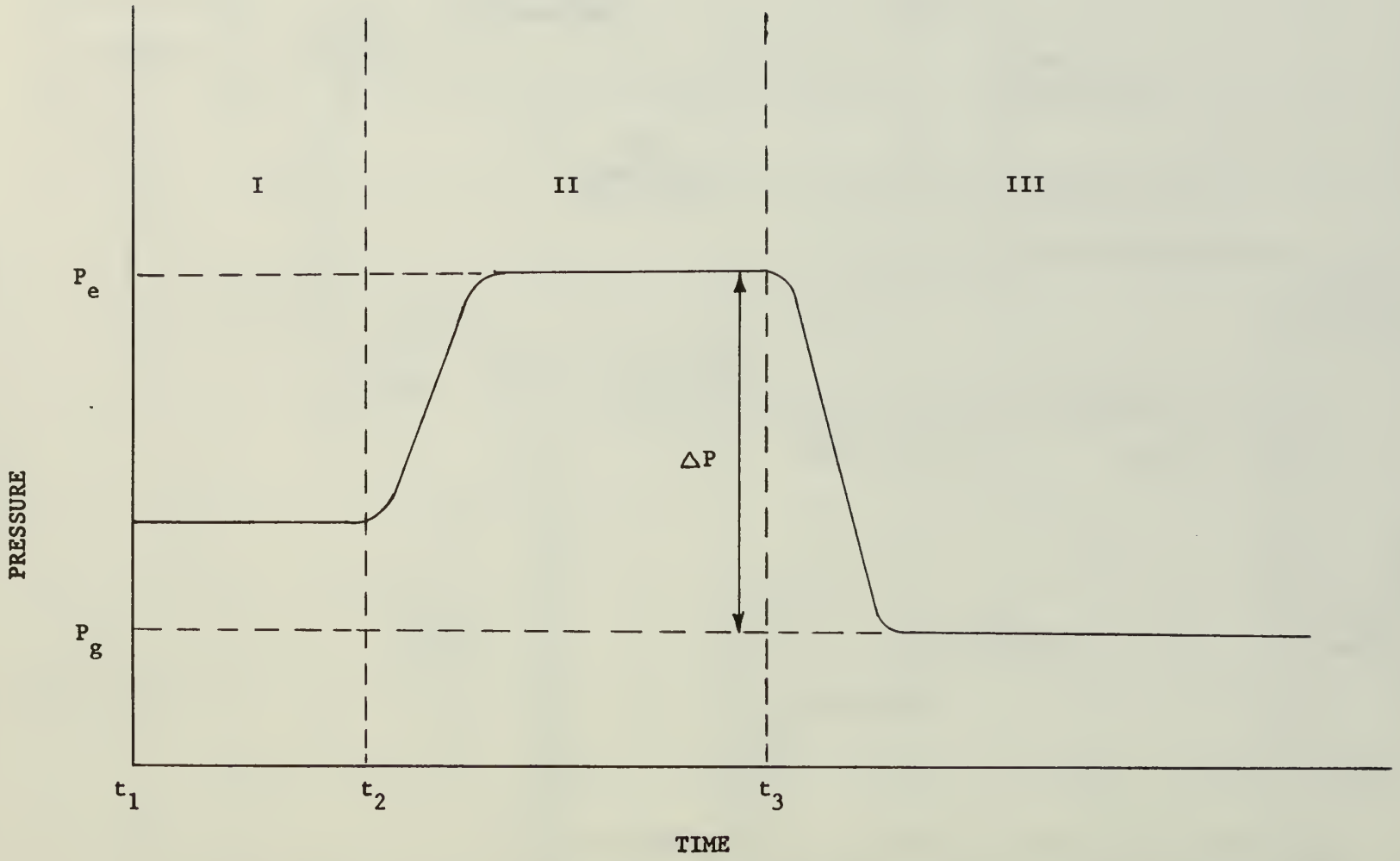

FIGURE 3 . PRESSURE VS. TIME(CONDENSABLE GAS ONLY)

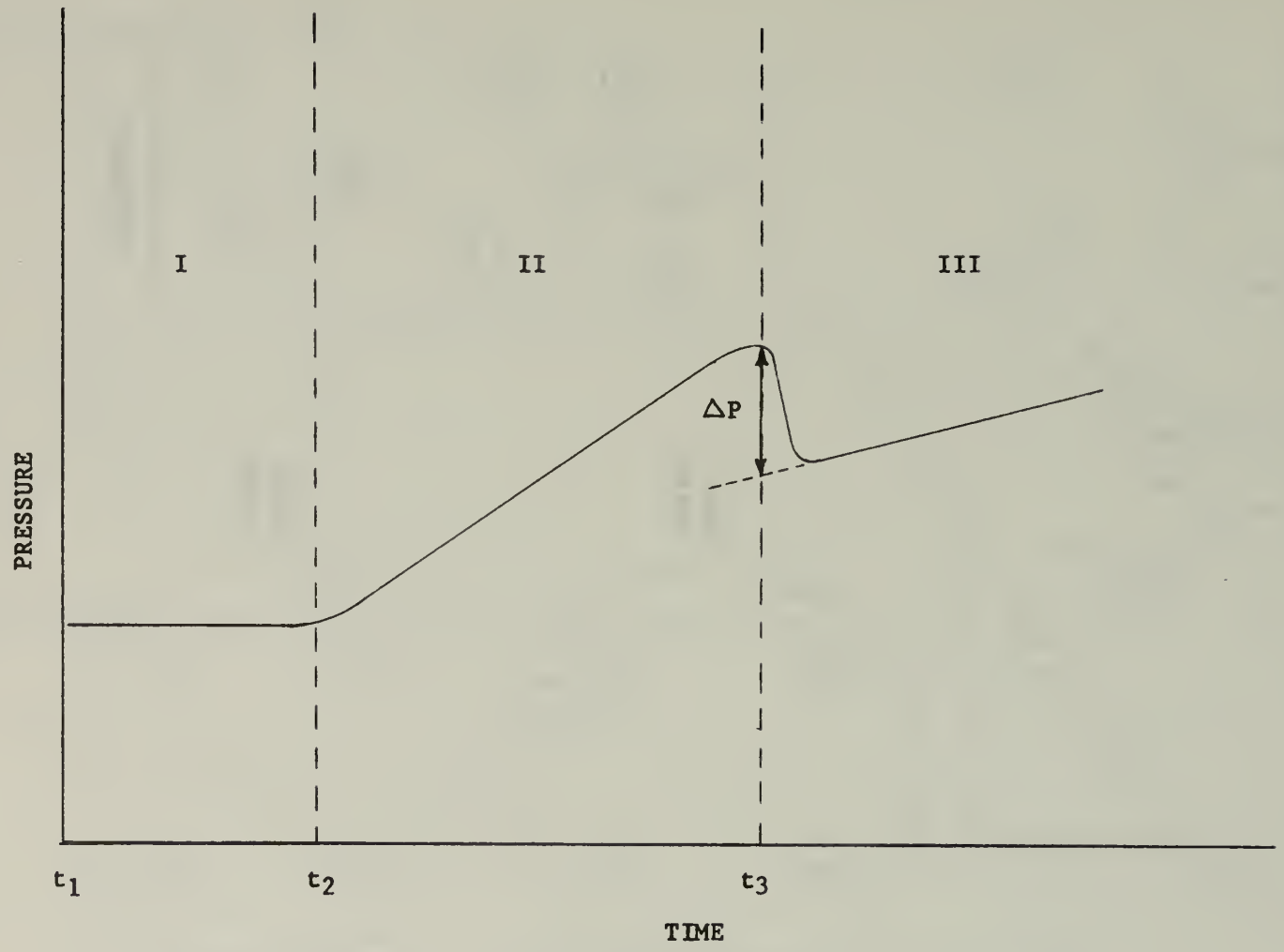

FIGURE 4. PRESSURE VS. TIME (CONDENSABLE AND NONCONDENSABLE GASES)

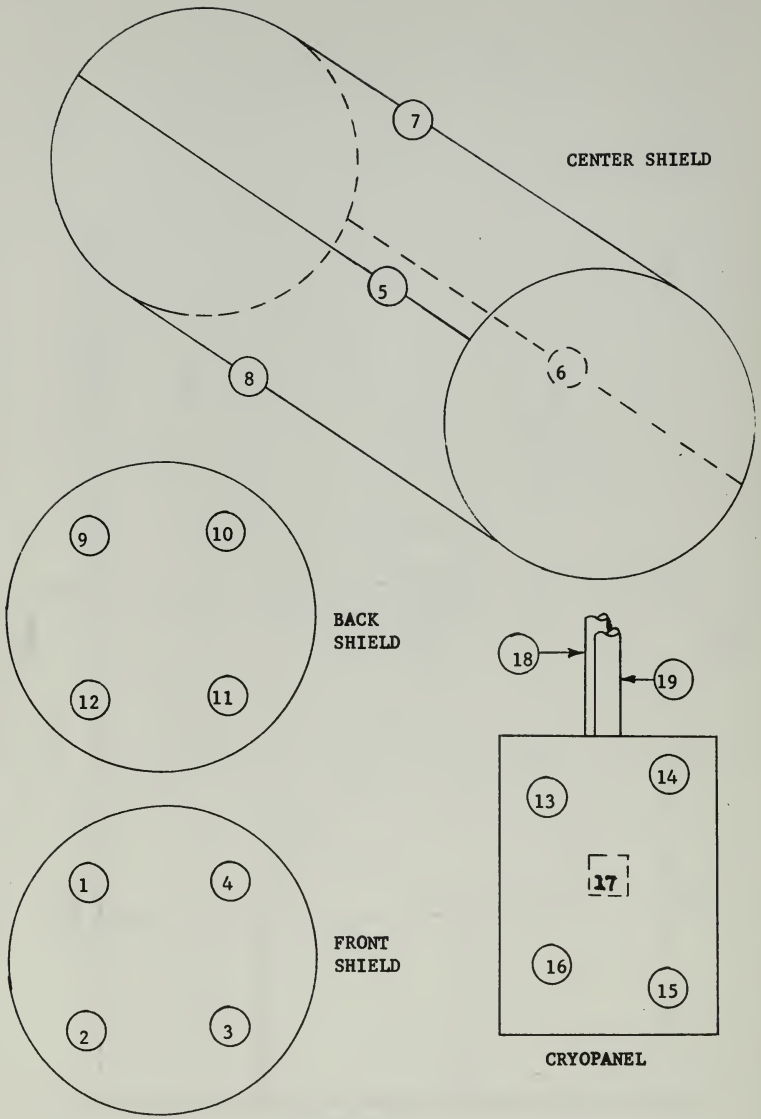

FIGURE 5. LOCATION OF THERMOCOUPLES

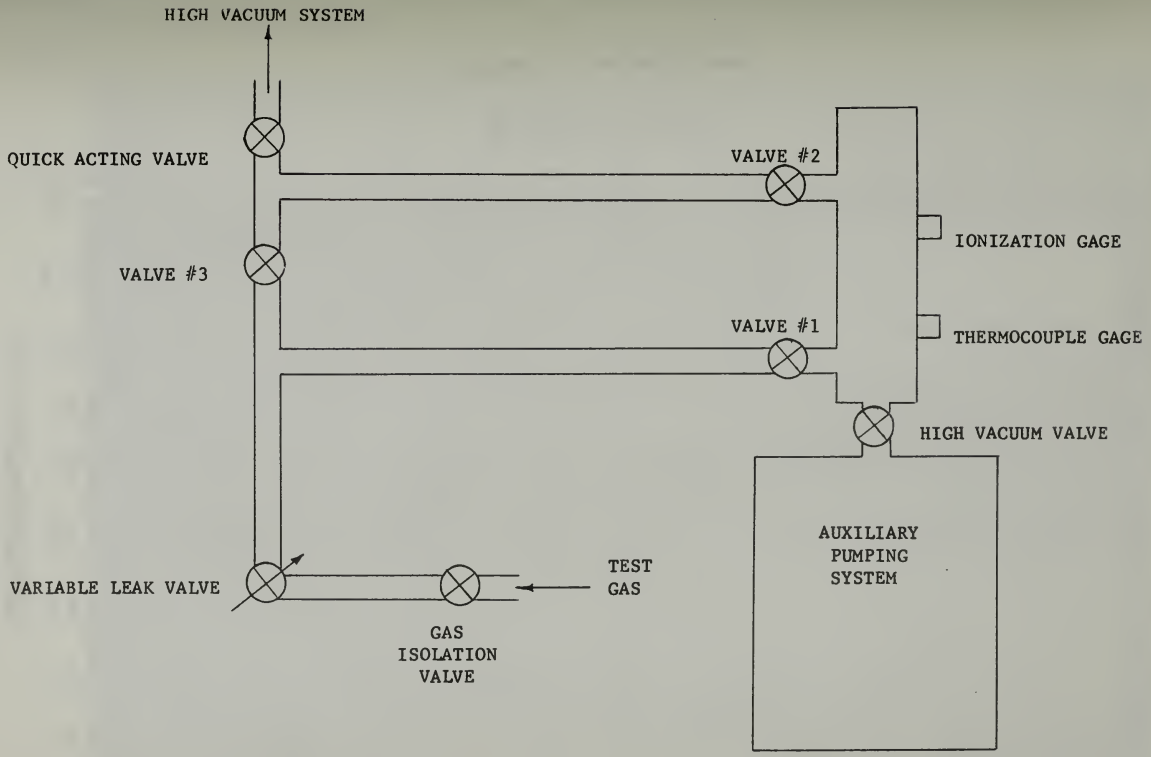

FIGURE 6 . GAS ADDITION AND FLOW MEASUREMENT SYSTEM

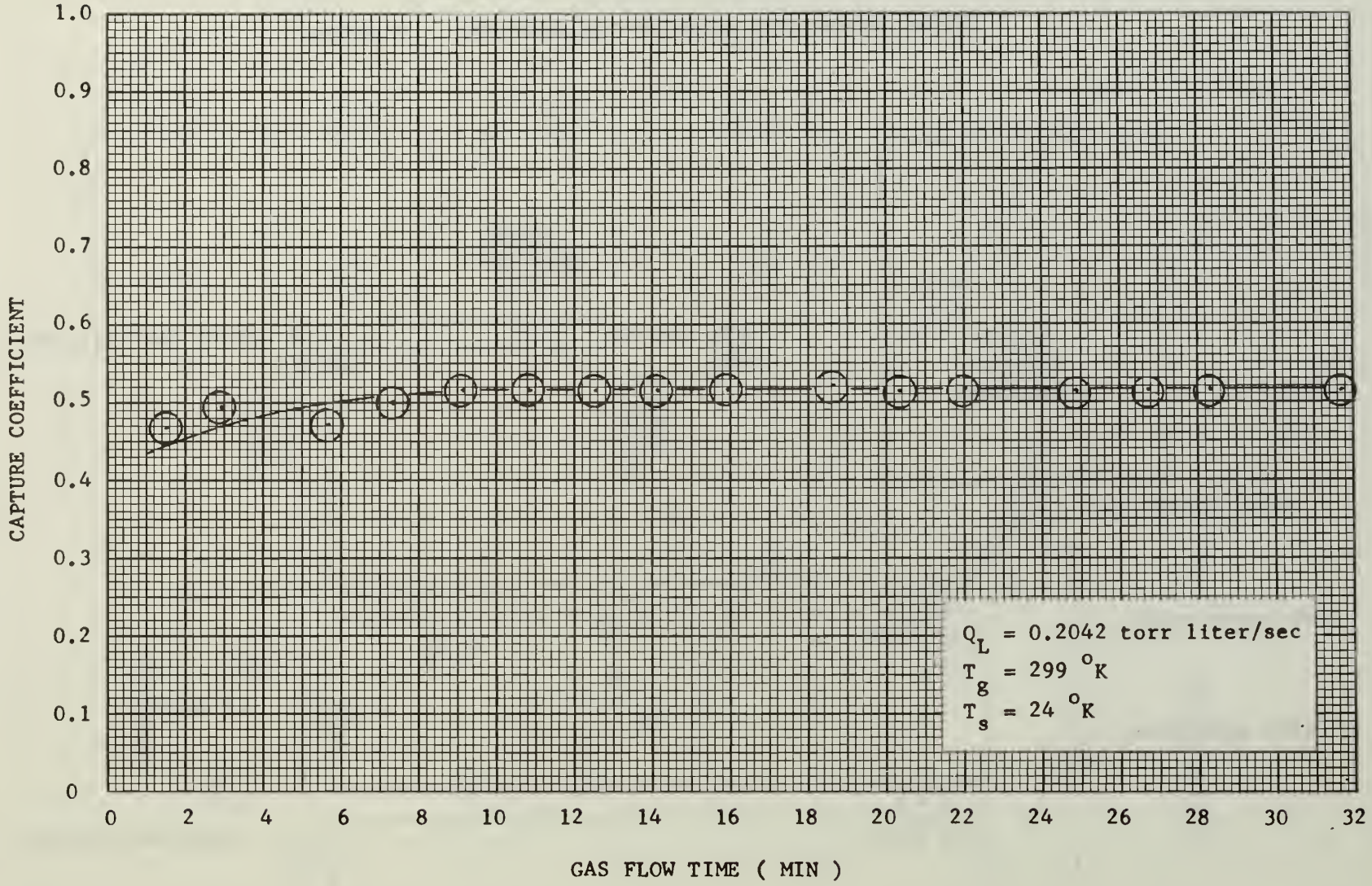

FIGURE 7. NITROGEN CURVE

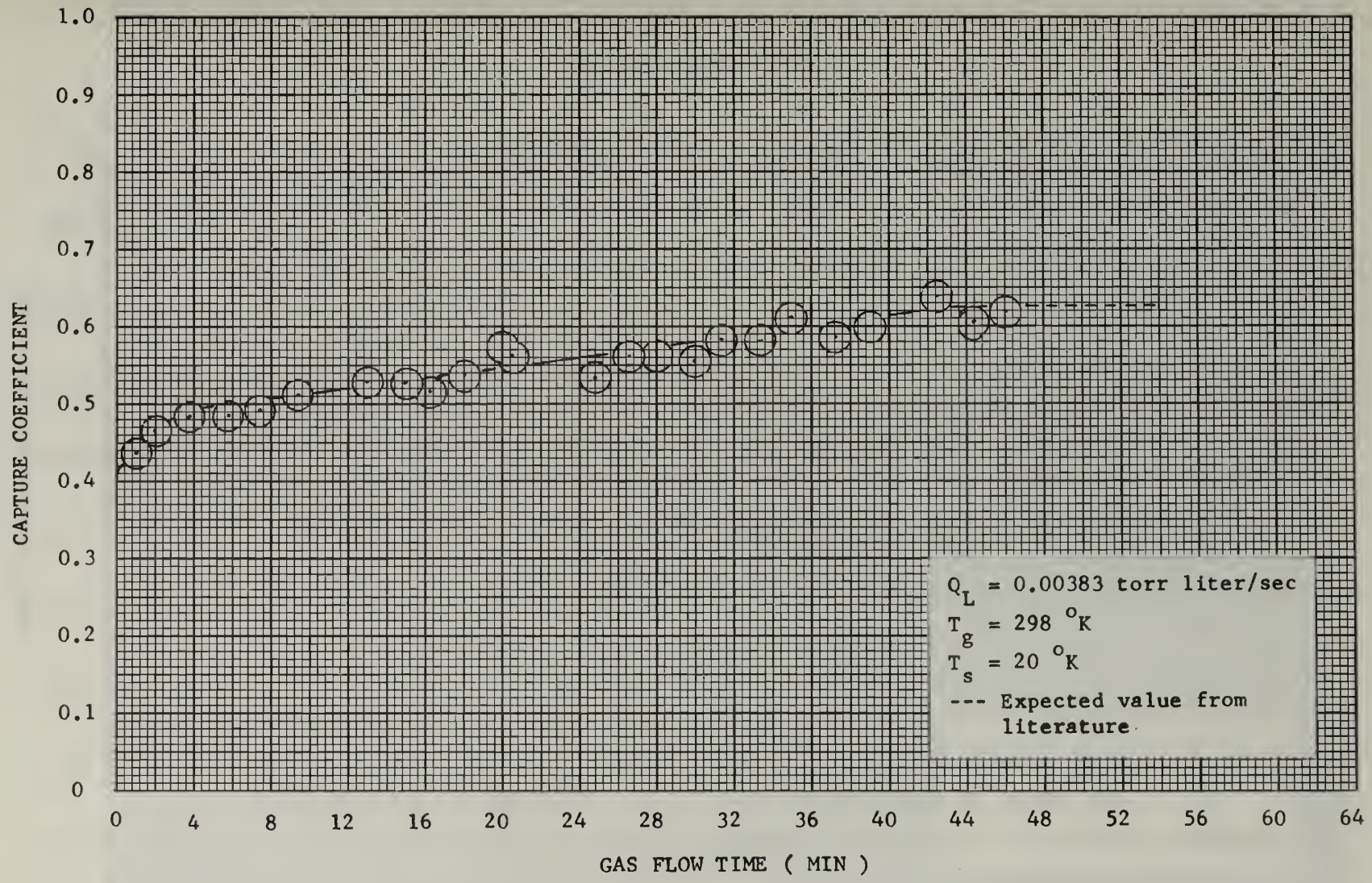

FIGURE 8. NITROGEN CURVE

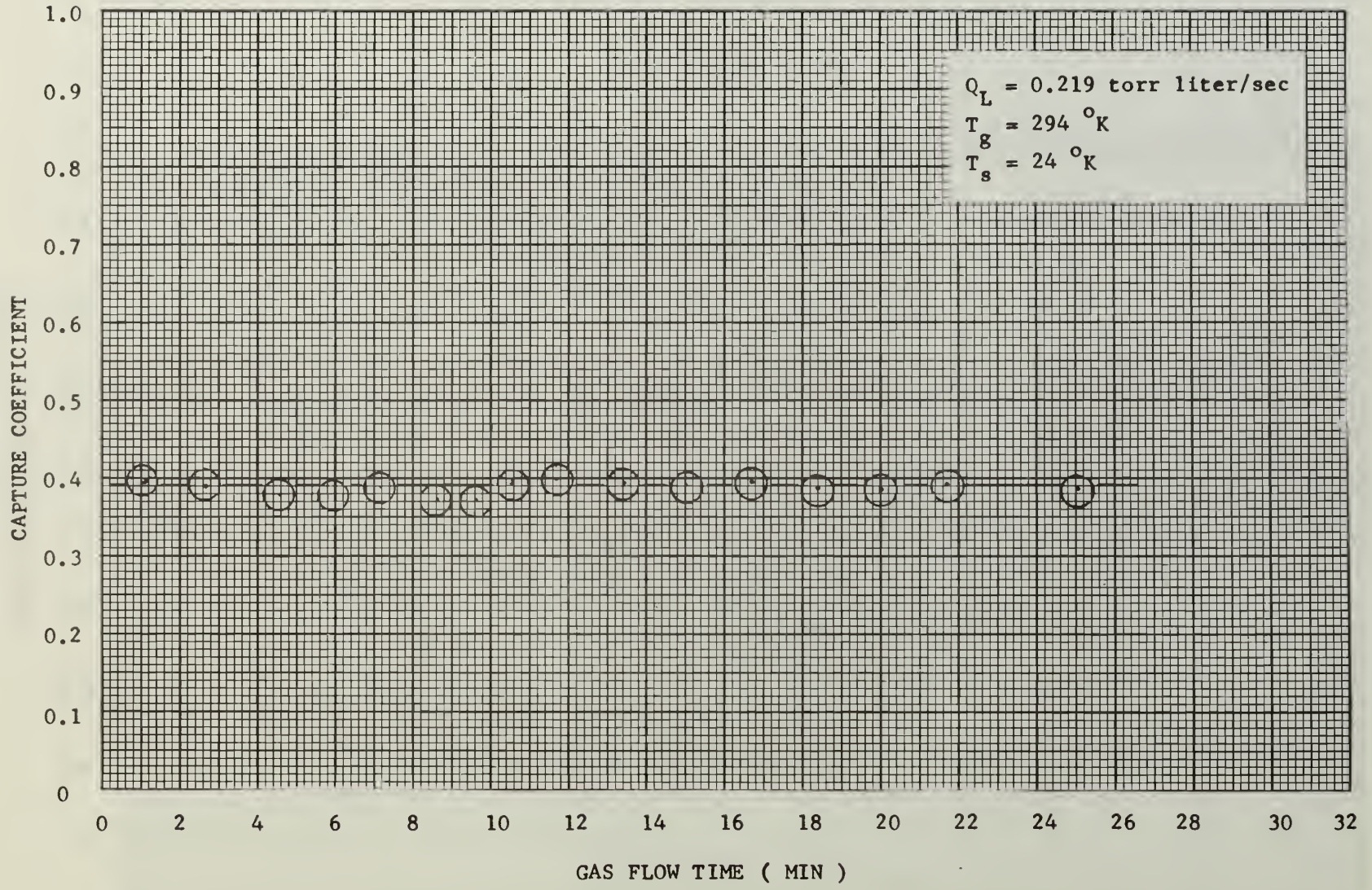

FIGURE 9. CARBON DIOXIDE CURVE

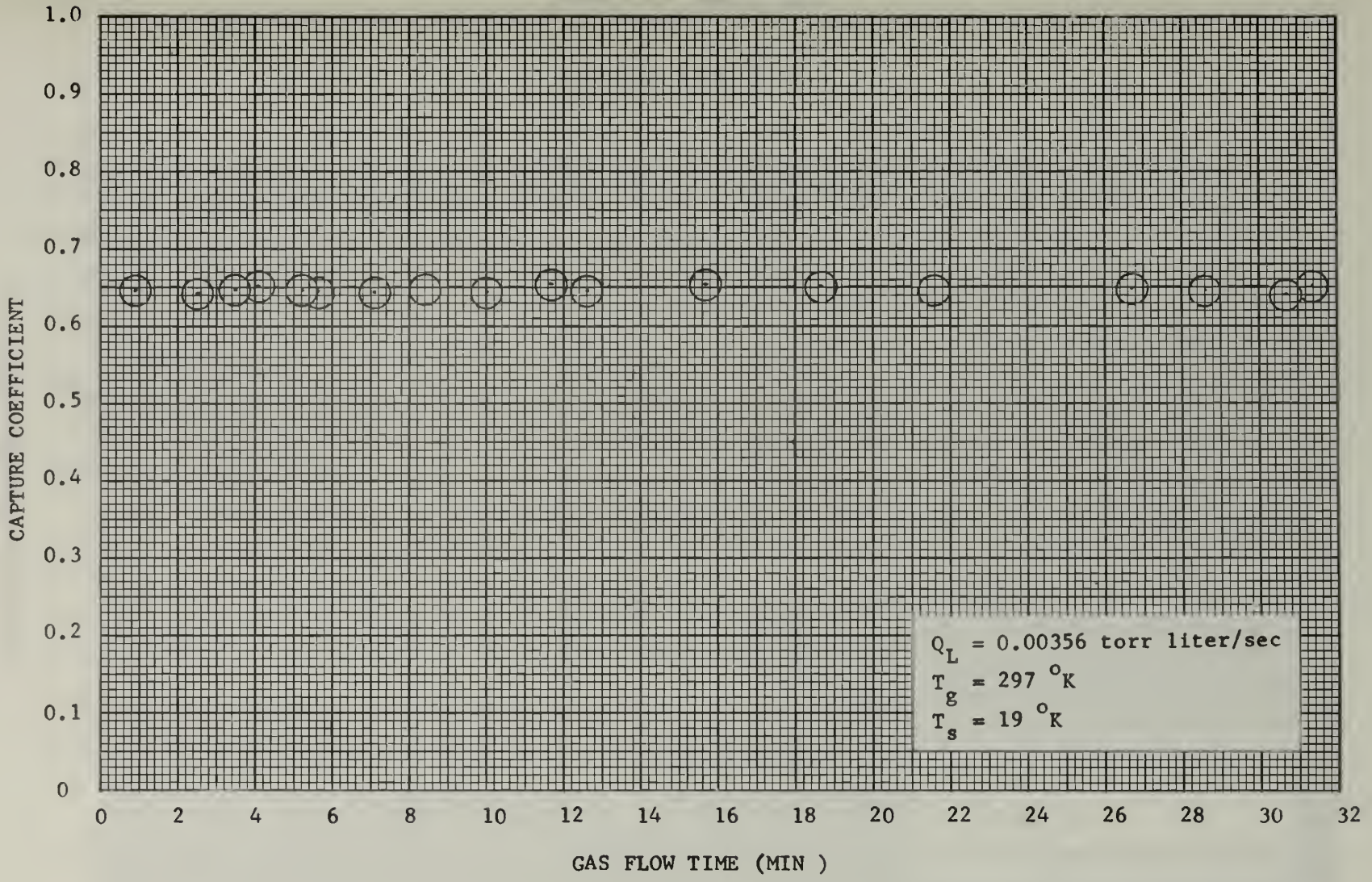

FIGURE 10. CARBON DIOXIDE CURVE

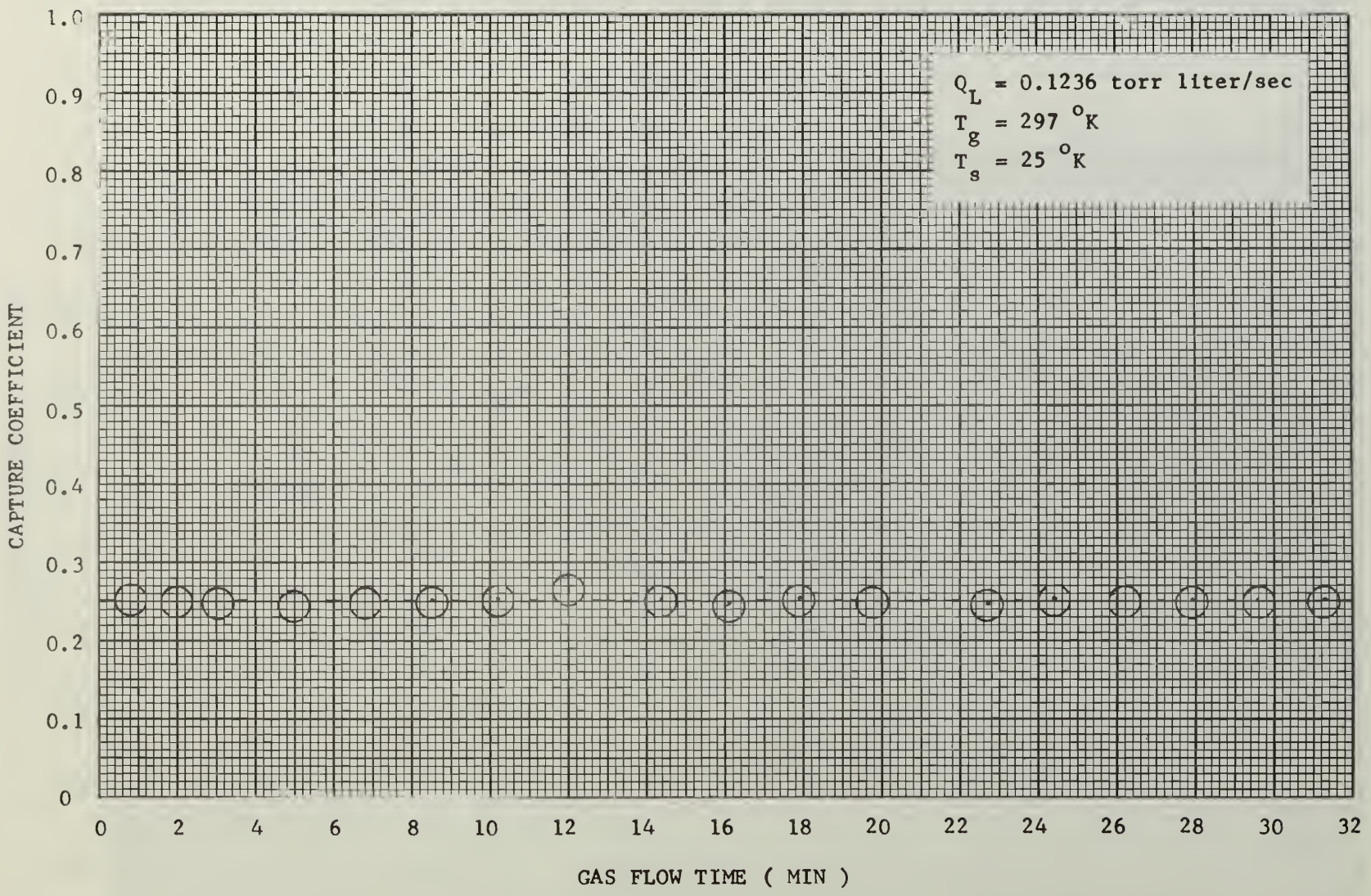

FIGURE 11. ARGON CURVE

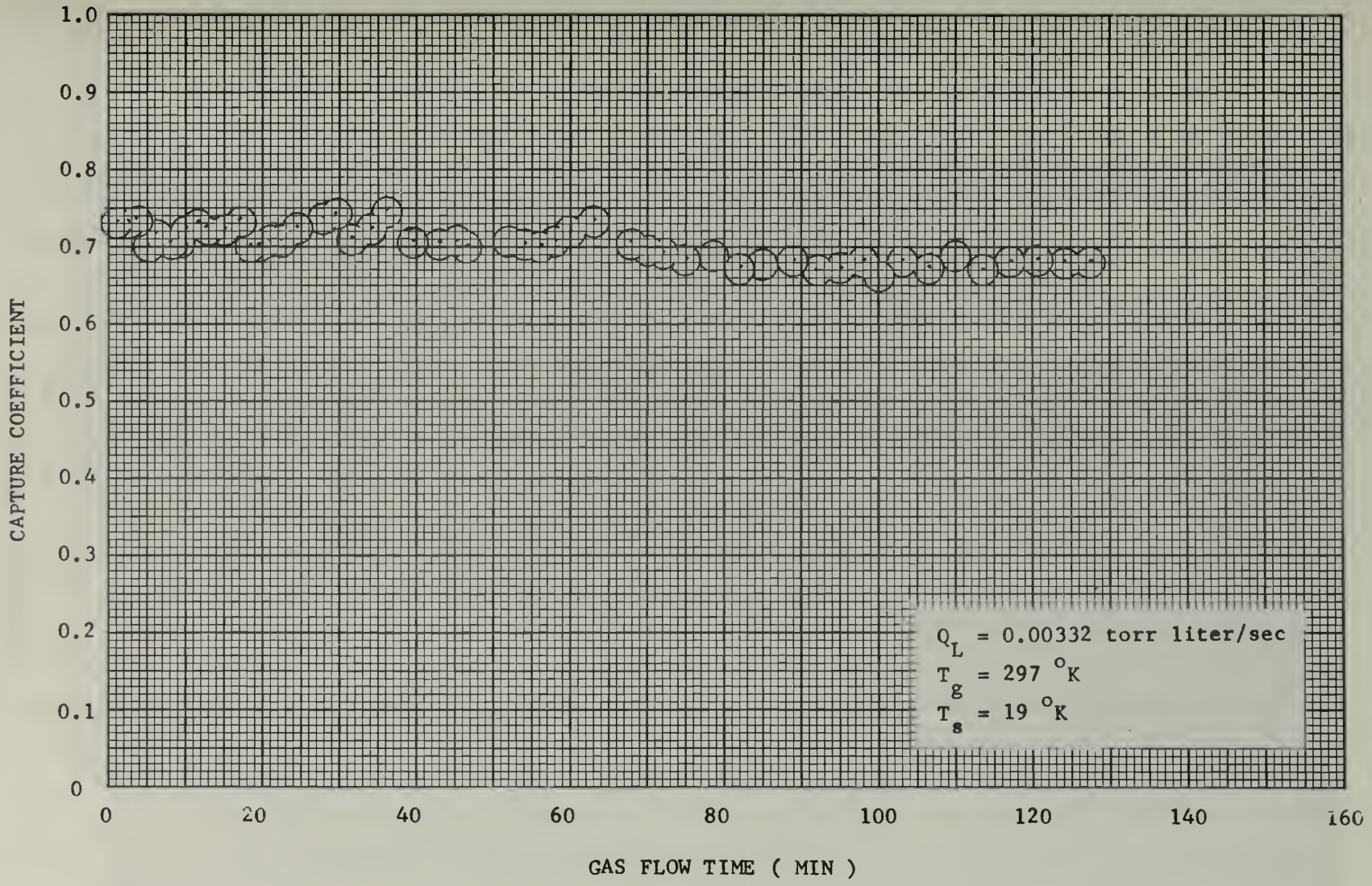

FIGURE 12. ARGON CURVE

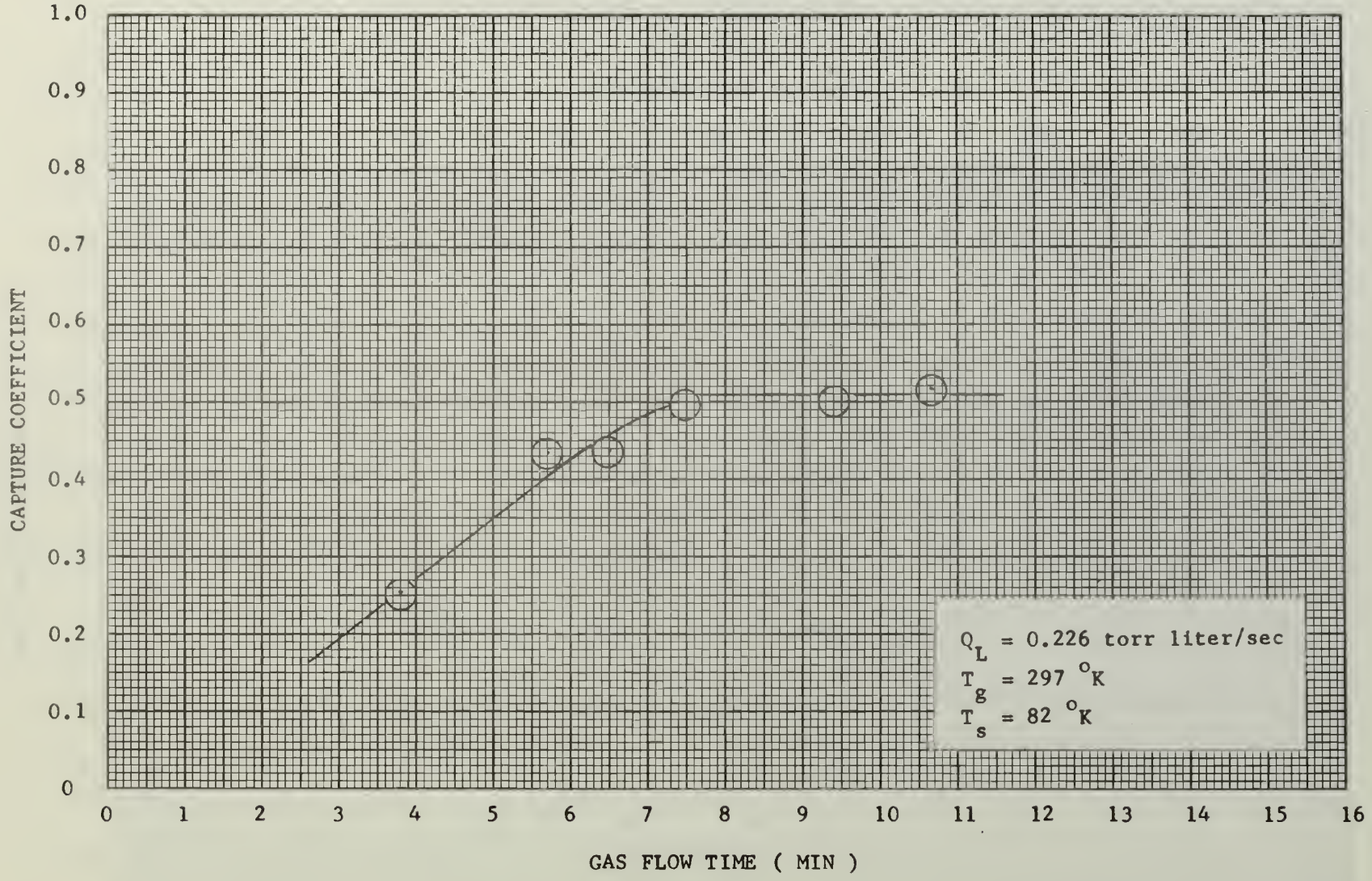

FIGURE 13. CARBON DIOXIDE CURVE

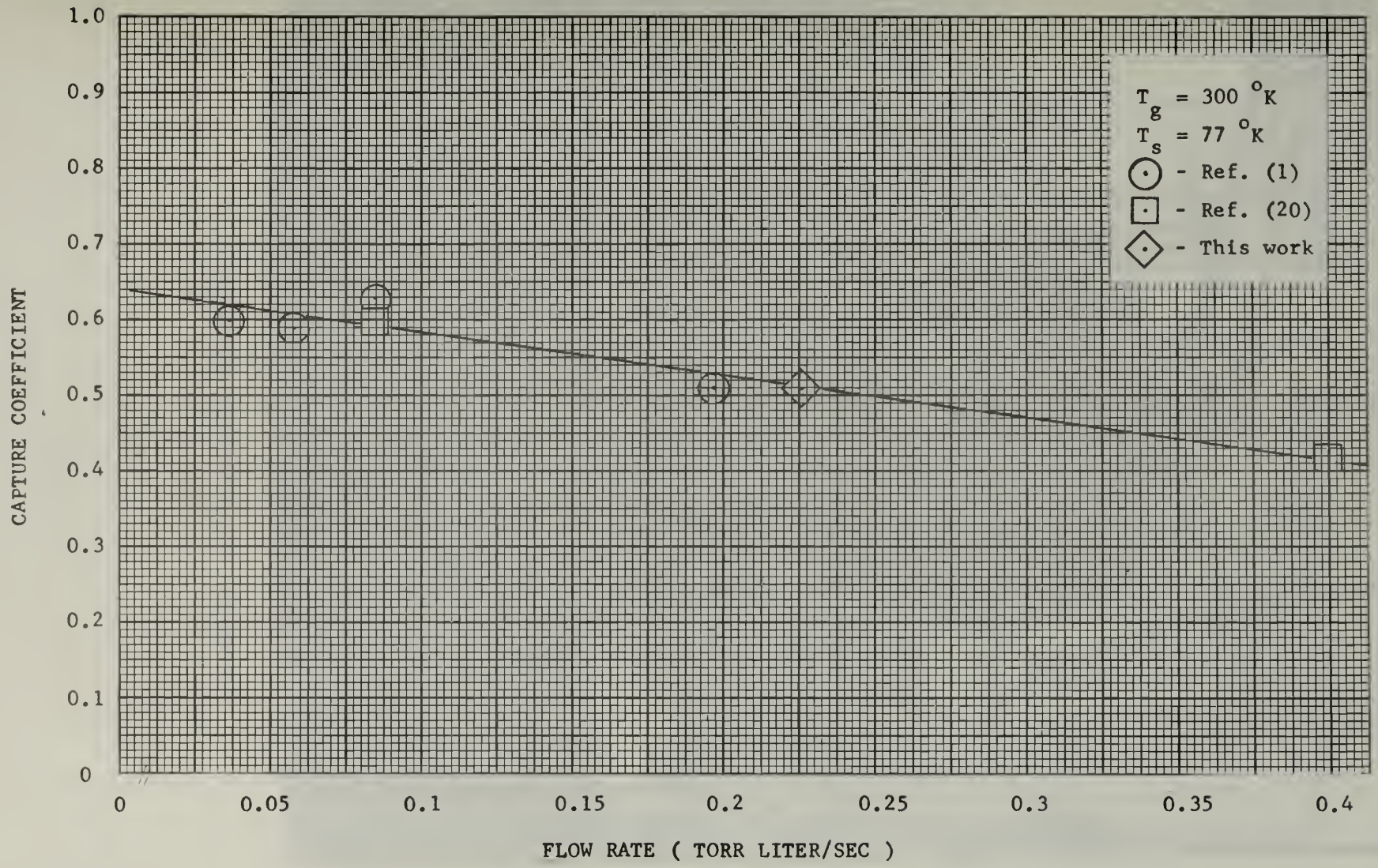

FIGURE 14. COMPARISON OF RESULTS FOR CARBON DIOXIDE

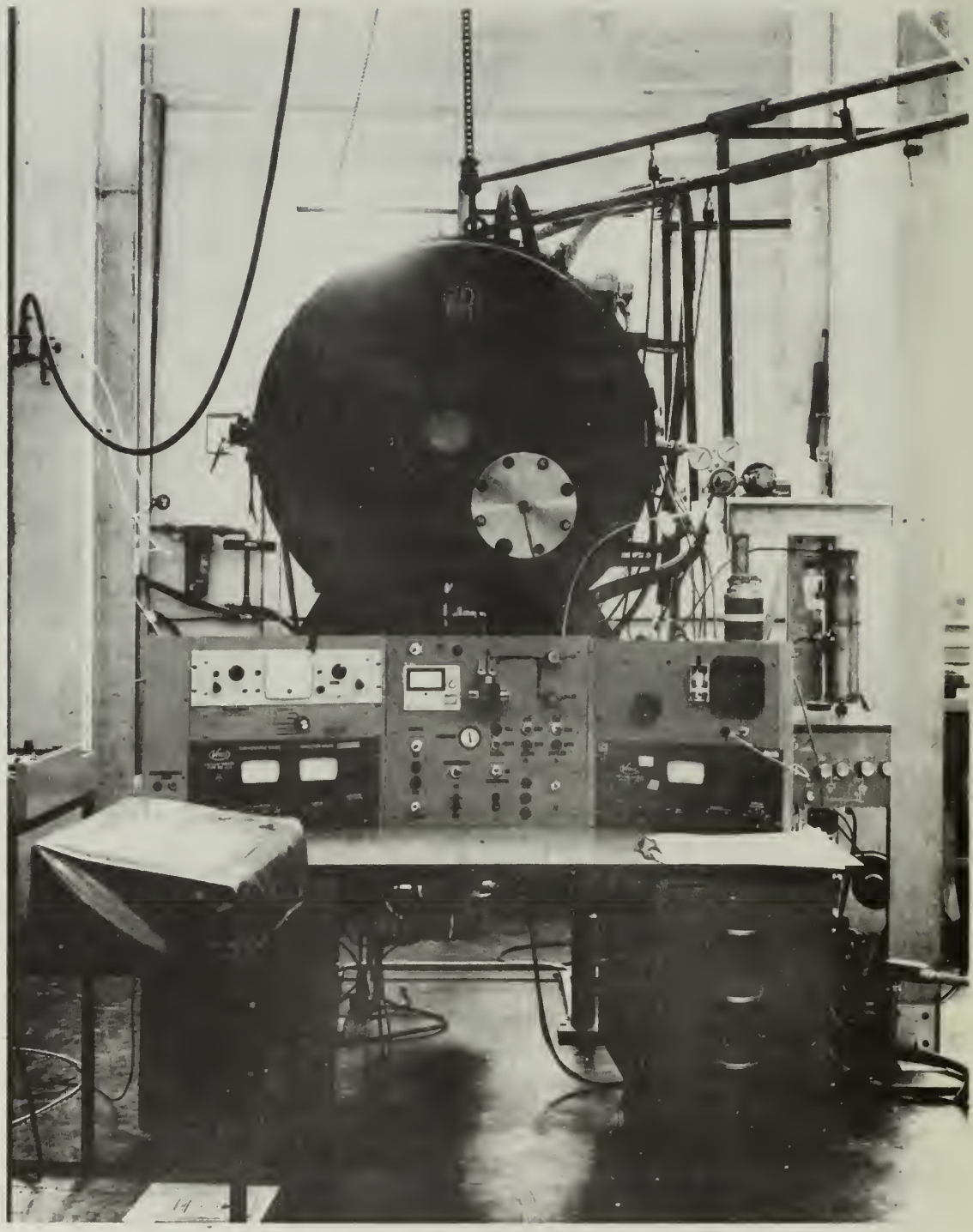

FIGURE 15. Front View of System

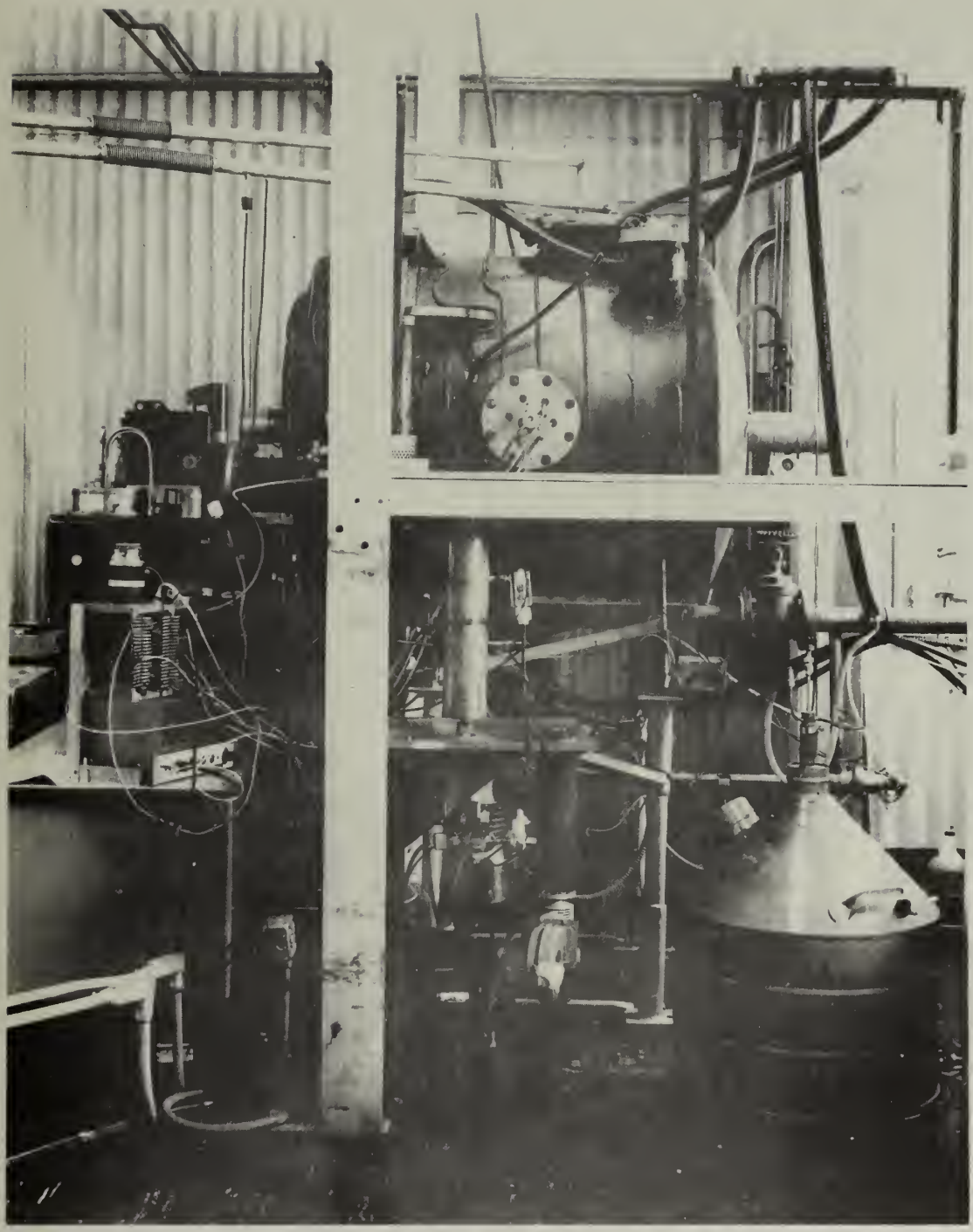

FIGURE 16. Side View of System

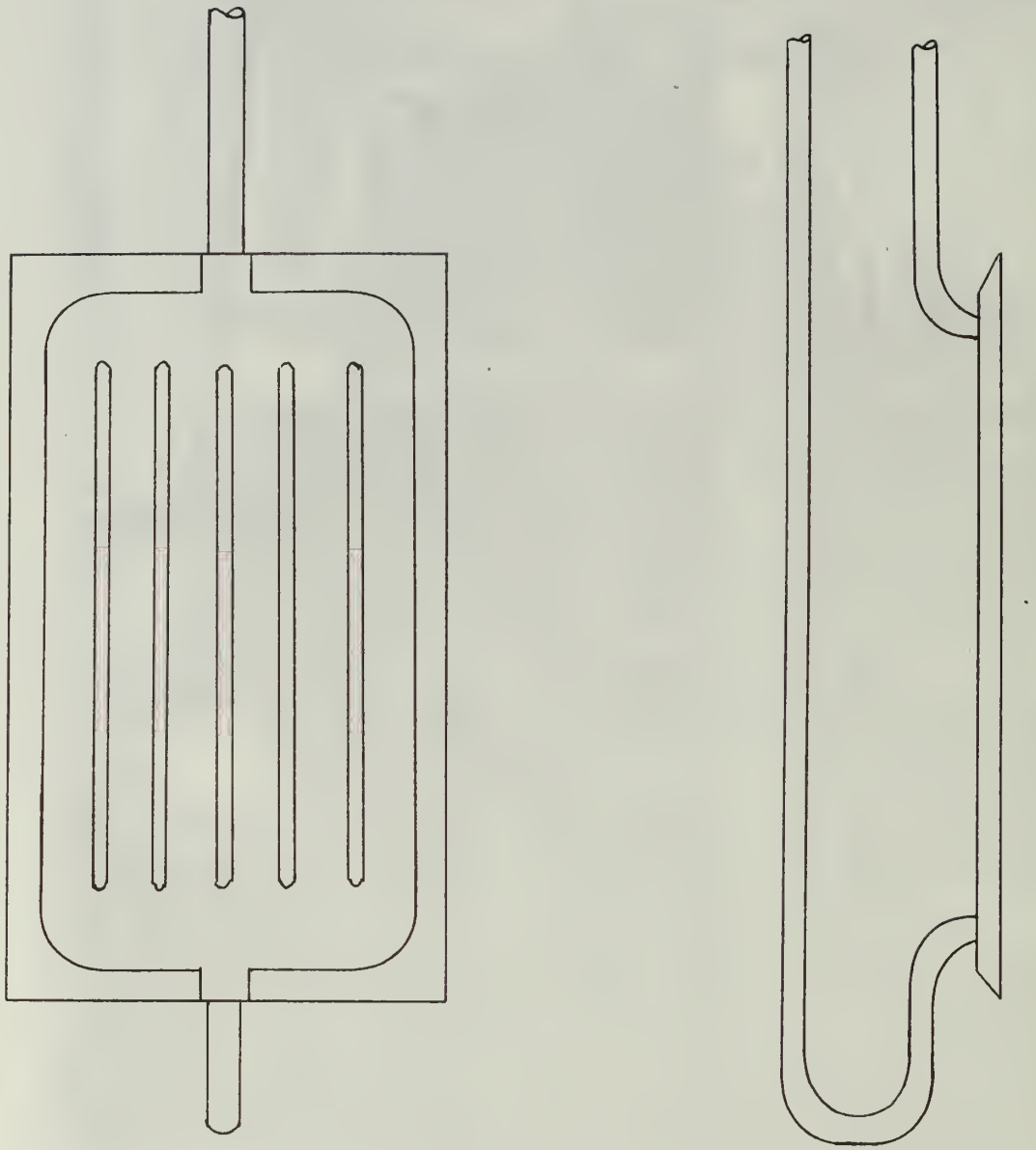

FIGURE 17. CRYOPANEL

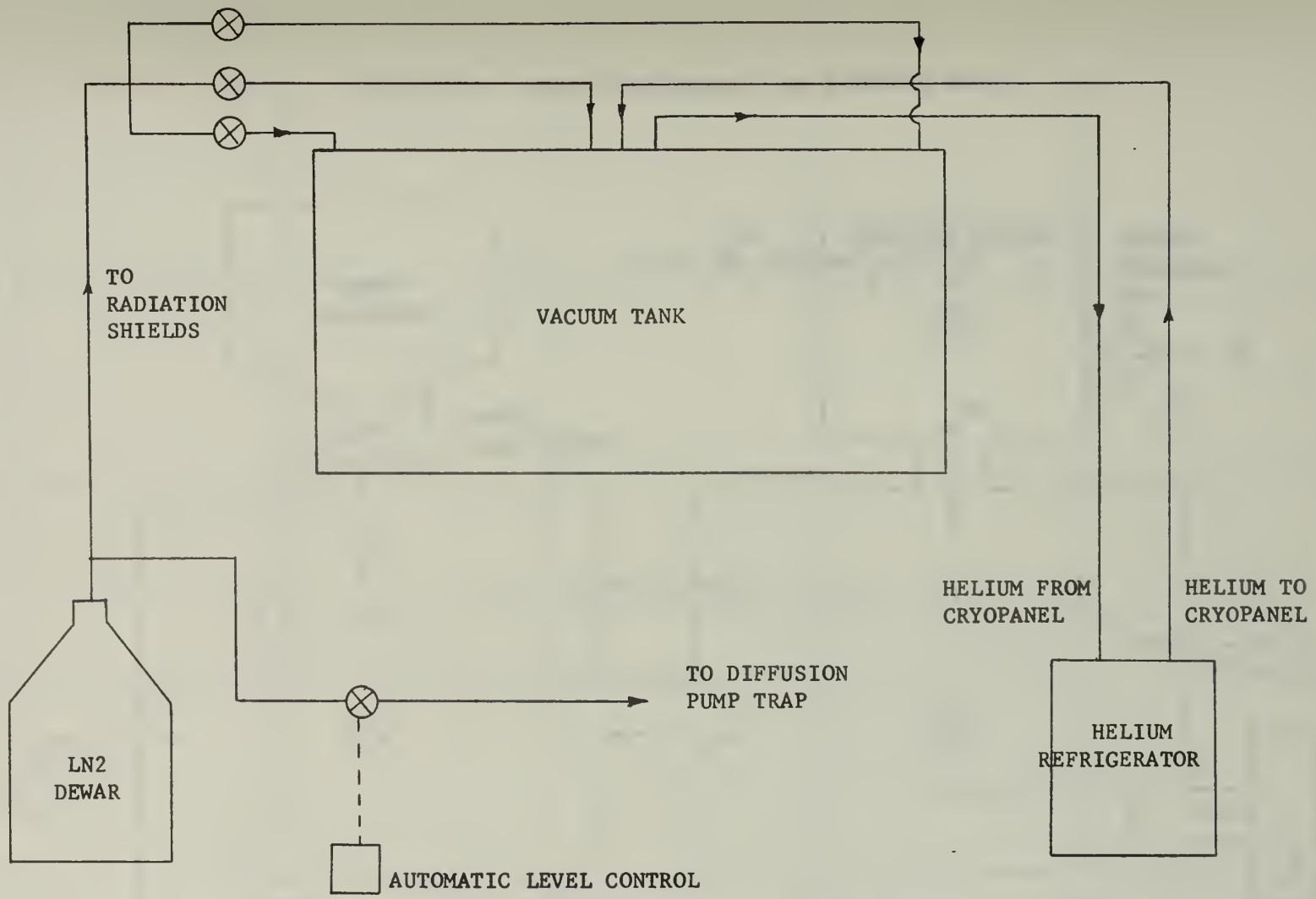

FIGURE 18. SCHEMATIC OF CRYOGENIC FLUID TRANSFER SYSTEM

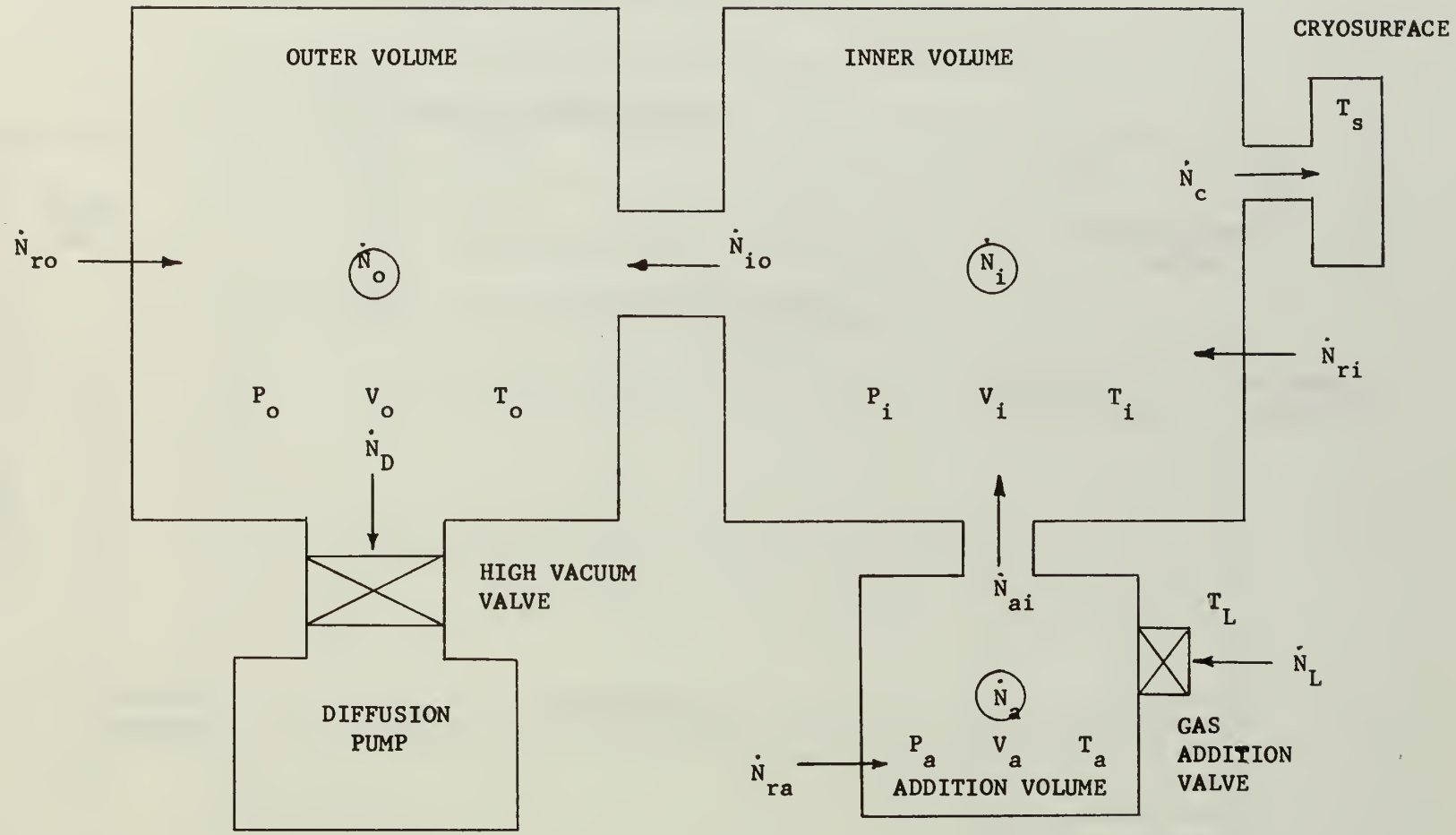

FIGURE 19 . MODEL FOR ANALYSIS OF PRESSURE DROP

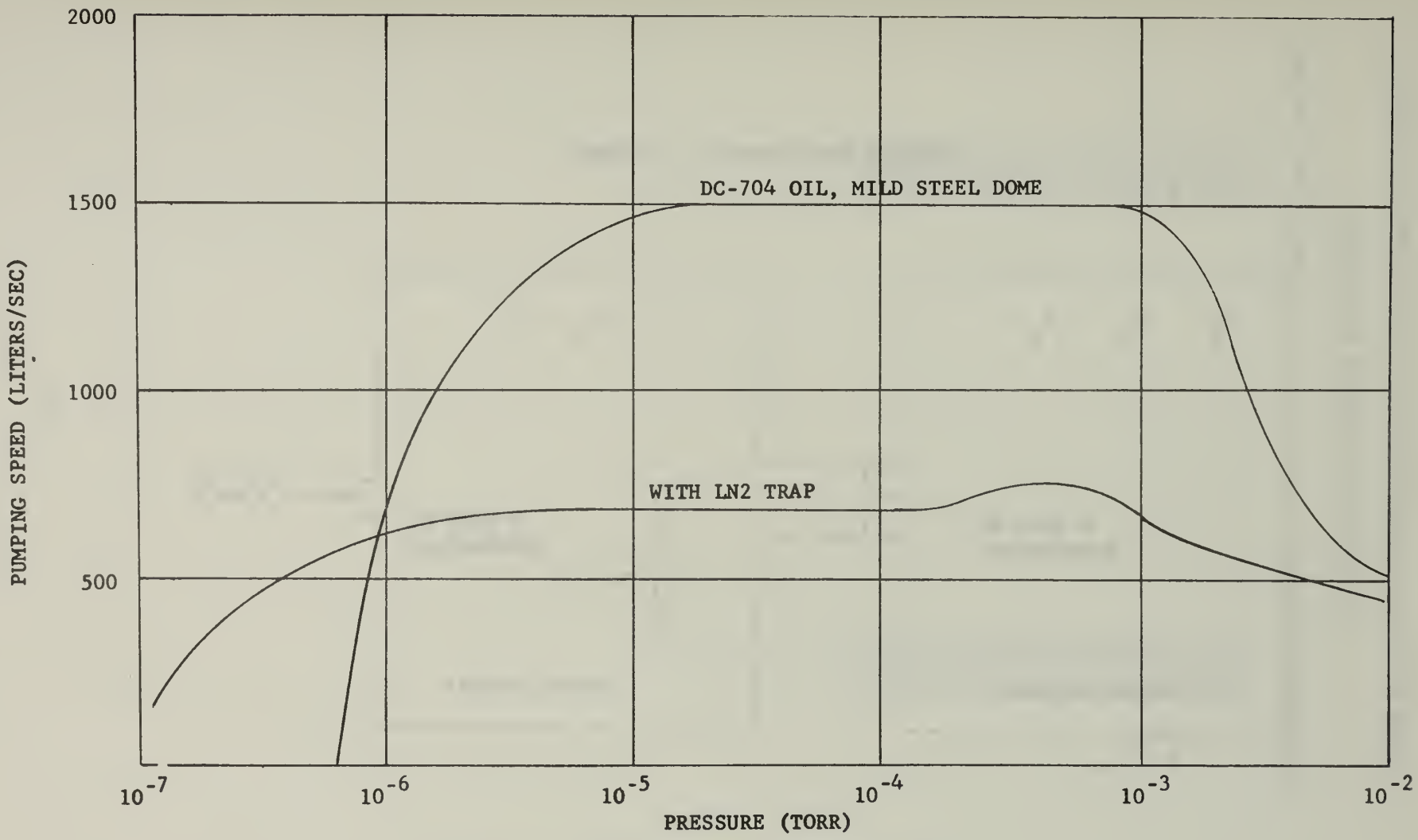

FIGURE 20. DIFFUSION PUMP CHARACTERISTICS

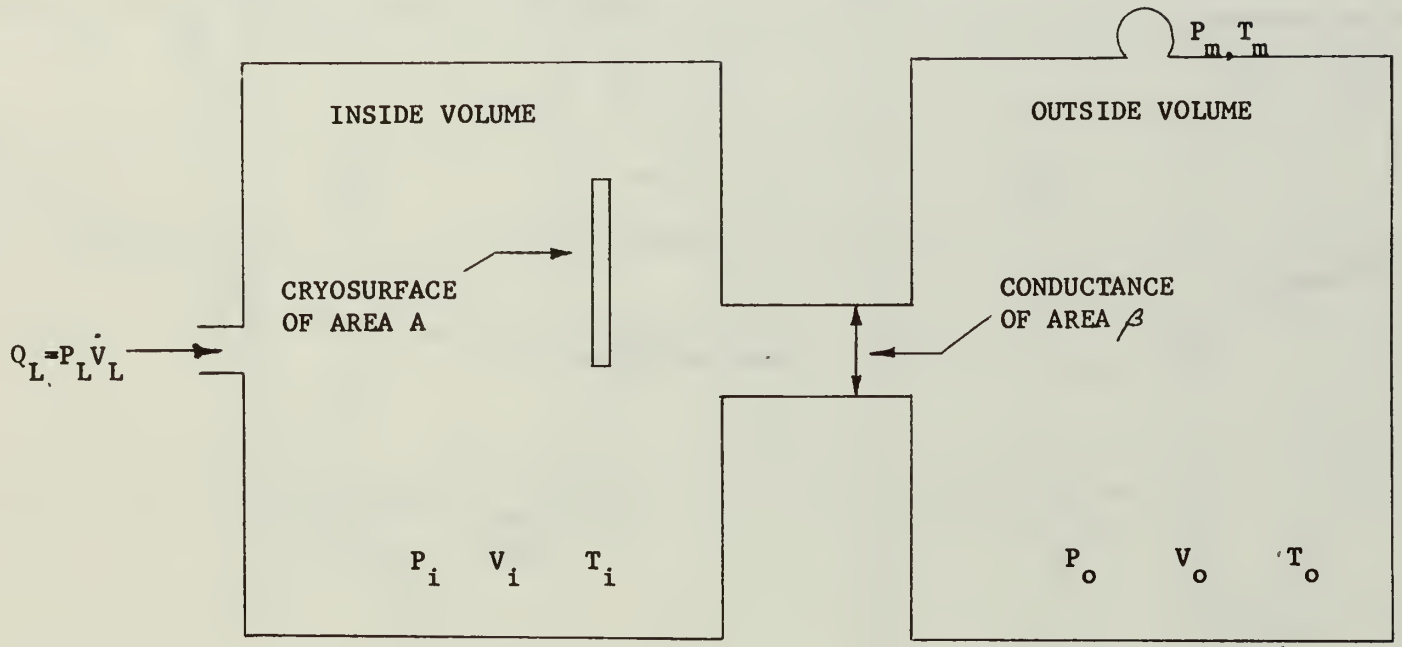

FIGURE 21. CONDUCTANCE EFFECTS

Table I. Experimental Data for Nitrogen with 24°K Panel

Flow Rate = 0.2042 torr liter/sec

Capture Coefficient	Gas Flow Time (min)
0.471	1.49
0.493	2.88
0.471	5.56
0.502	7.30
0.518	9.10
0.519	10.82
0.518	12.53
0.517	14.20
0.517	15.90
0.517	18.57
0.517	20.29
0.517	22.00
0.517	24.89
0.517	26.68
0.517	28.38
0.516	31.79

Table II. Experimental Data for Nitrogen with 20°K Panel

Flow Rate = 0.00383 torr liter/sec

Capture Coefficient	Gas Flow Time (min)
0.438	1.09
0.467	2.05
0.484	3.83
0.486	5.81
0.493	7.63
0.511	9.51
0.531	13.08
0.527	14.80
0.518	16.34
0.539	18.13
0.574	19.83
0.562	21.53
0.533	24.86
0.561	26.60
0.561	28.28
0.559	29.93
0.583	31.63
0.581	33.48
0.612	35.16
0.587	37.29
0.601	39.03
0.640	42.49
0.609	44.34
0.620	46.16

Table III. Experimental Data for Carbon Dioxide with 24°K Panel

Flow Rate = 0.219 torr liter/sec

Capture Coefficient	Gas Flow Time (min)
0.395	1.09
0.389	2.73
0.383	4.63
0.381	5.97
0.386	7.24
0.373	8.60
0.371	9.56
0.394	10.59
0.402	11.68
0.395	13.36
0.393	15.04
0.395	16.73
0.389	18.36
0.387	20.04
0.392	21.69
0.388	25.06

Table IV. Experimental Data for Carbon Dioxide with 19°K Panel

Flow Rate = 0.00356 torr liter/sec

Capture Coefficient	Gas Flow Time (min)
0.647	0.92
0.642	2.49
0.647	3.53
0.652	4.07
0.647	5.17
0.647	5.66
0.644	7.15
0.650	8.43
0.644	9.98
0.655	11.68
0.647	12.62
0.655	15.67
0.652	18.72
0.647	21.59
0.650	26.66
0.647	28.63
0.642	30.66
0.652	31.39
0.642	33.21
0.650	34.49
0.652	37.41
0.661	39.43
0.655	40.21

Table V. Experimental Data for Argon with 25°K Panel

Flow Rate = 0.1236 torr liter/sec

Capture Coefficient	Gas Flow Time (min)
0.257	0.80
0.253	1.98
0.252	3.05
0.246	5.07
0.252	6.78
0.251	8.46
0.254	10.24
0.267	11.96
0.253	14.41
0.248	16.12
0.253	17.85
0.251	19.82
0.248	22.68
0.253	24.38
0.252	26.15
0.253	27.88
0.252	29.62
0.252	31.32
0.252	33.05

Table VI. Experimental Data for Argon with 19°K Panel

Flow Rate = 0.00332 torr liter/sec

Capture Coefficient	Gas Flow Time (min)	Capture Coefficient	Gas Flow Time (min)
0.733	1.12	0.712	52.57
0.733	2.67	0.707	54.37
0.738	3.40	0.702	56.19
0.703	5.20	0.711	58.09
0.720	5.73	0.724	60.11
0.707	8.00	0.737	62.91
0.711	9.19	0.707	68.10
0.724	10.14	0.699	70.27
0.732	11.27	0.695	72.62
0.728	12.47	0.687	75.13
0.724	15.05	0.690	78.59
0.738	16.77	0.675	81.72
0.702	18.27	0.679	85.20
0.706	19.61	0.683	89.37
0.710	21.00	0.671	91.74
0.710	22.67	0.675	94.98
0.728	24.48	0.683	91.71
0.741	27.81	0.667	100.1
0.745	29.60	0.686	103.3
0.714	31.51	0.674	106.6
0.723	34.12	0.690	110.1
0.750	35.89	0.671	113.4
0.709	39.67	0.682	116.9
0.709	43.24	0.686	120.4
0.710	45.31	0.683	123.8
0.702	46.85	0.682	127.2

Table VII. Experimental Data for Carbon Dioxide with 82°K Panel

Flow Rate = 0.226 torr liter/sec

Capture Coefficient	Gas Flow Time (min)
0.435	5.68
0.439	6.54
0.501	7.52
0.506	9.43
0.517	10.65

Table VIII. Reported Capture Coefficients of Nitrogen

Gas Temperature in °K	Cryosurface Temperature in °K	Flow Rate in torr liter per second	Capture Coefficient	Reference
300	10	Not Reported	0.66	8
300	20	Not Reported	0.61	8
300	20	Not Reported	0.60	9
294	33	Variable	0.65	18
300	25	0.00226	0.62	3
298	20	0.00383	0.63	This Work
300	25	0.22	0.42	3
299	24	0.2042	0.52	This Work

Table IX. Reported Capture Coefficients of Carbon Dioxide

Gas Temperature in °K	Cryosurface Temperature in °K	Flow rate in torr liter per second	Capture Coefficient	Reference
300	10	Not Reported	0.77	8
300	10	Not Reported	0.75	9
300	20	Not Reported	0.62	8
300	20	Not Reported	0.63	9
300	20	Not Reported	0.64	7
297	19	0.00356	0.65	This Work
294	24	0.219	0.39	This Work
300	86	Variable	0.58	18
300	77	Not Reported	0.63	9
300	77	Not Reported	0.62	4
300	77	0.084	0.63*	1
300	77	0.0798	0.60	20
297	82	0.226	0.51	This Work
300	77	0.399	0.42	20
300	77	0.1975	0.51*	1

*Corrected

Table X. Reported Capture Coefficients of Argon

Gas Temperature in °K	Cryosurface Temperature in °K	Flow Rate in torr liter per second	Capture Coefficient	Reference
300	10	Not Reported	0.68	8
300	20	Not Reported	0.65	8
300	20	Not Reported	0.66	9
297	19	0.00332	0.68	This Work
297	25	0.1236	0.25	This Work

Table XI. Reported Observations of the Bare Surface Effect

Gas	Gas Temp.°K	Cryopanel Temp.°K	Comment	Reference
CO_2	300	77	Q_L = 0.5 torr liter sec^{-1}	20
CO_2	300	77	Q_L = 0.0572 torr liter sec^{-1}	1
CO_2	300	77	No observed bare surface effect	5
CO_2	297	82	Q_L = 0.226 torr liter sec^{-1}	*
CO_2	294	24	Q_L = 0.219 torr liter sec^{-1} No observed bare surface effect	*
CO_2	297	19	Q_L = 0.00356 torr liter sec^{-1} No observed bare surface effect	*
N_2	79	18	Flow rate not applicable due to experimental method	17
N_2	299	24	Q_L = 0.2042 torr liter sec^{-1}	*
N_2	298	20	Q_L = 0.00383 torr liter sec^{-1}	*
H_2	300	3	Flow rate not specified	6
A	297	25	Q_L = 0.1236 torr liter sec^{-1} No observed bare surface effect	*
A	297	19	Q_L = 0.00332 torr liter sec^{-1} No observed bare surface effect	*
CO_2, N_2, A, N_2O, CO			Made preliminary coating of frost to eliminate bare surface effect	8

*This work

Table XII. Uncertainties in Measured Values

Quantity	Value	Uncertainty	$\frac{\Delta x}{x}$
V_L	4350 cm^3	30 cm^3	0.007
A_S	3300 cm^2	50 cm^2	0.015
$\gamma\beta$	7780 cm^2	500 cm^2	0.064
T_L	300°K	2°K	0.007
T_g	300°K	2°K	0.007
ΔP	Variable	- - -	0.020
$\dot{P}_L$	Variable	- - -	0.095

COEFFICIENT	EXPRESSION	COEFFICIENT	EXPRESSION
A	$\frac{Q_{ri}}{V_i} + \frac{f_s A_s T_i}{V_i}\left[\frac{k}{2\pi m T_s}\right]^{\frac{1}{2}} P_s$	a_4	$\frac{f_g A_s}{V_i}\left[\frac{k T_i}{2\pi m}\right]^{\frac{1}{2}}$
B	$\frac{Q_{ro}}{V_o}$	a_5	$\frac{C_i k T_i^{\frac{1}{2}}}{V_i}$
C	$\frac{Q_{ra}}{V_a}$	a_6	$\frac{C_i k T_o}{V_o T_i^{1/2}}$
D	$\frac{Q_L T_a}{V_a T_L}$	a_7	$\frac{\propto \dot{V}_o}{V_o}$
a_1	$\frac{C_i k T_i}{V_i T_o^{1/2}}$	a_8	$\frac{C_i k T_o^{\frac{1}{2}}}{V_o}$
a_2	$\frac{C_a k T_i}{V_i T_a^{1/2}}$	a_9	$\frac{C_a k T_a}{V_a T_i^{1/2}}$
a_3	$\frac{C_a k T_i^{1/2}}{V_i}$	a_{10}	$\frac{C_a k T_a^{1/2}}{V_a}$

TABLE XIII. COEFFICIENTS OF SYSTEM EQUATIONS

APPENDIX A

General Description of the System

The system described here was built and modified by several investigators (1,3,14,18). Photographs and schematics are included as Figures 2, 15, 16, and 17.

(a) Main Vacuum Chamber.

The vacuum chamber is a modified 40 inch diameter vacuum furnace manufactured by National Research Corporation. The modification was done by LaChance and is described in detail in his work (14). The chamber volume is 994 liters.

(b) Radiation Shielding.

The radiation shield is a 33 inch diameter, 36 inch long, type 304 stainless steel cylindrical shell with two 36 inch diameter end shields. They are singly embossed on the outer surface with fill and vent lines rising through a flange at the top of the chamber. All the shields were manufactured by Dean Products, Inc., Brooklyn, New York. The volumetric capacity of the entire shield is 33 liters and requires about 65 liters for an initial fill of liquid nitrogen.

(c) Cryopanel.

The cryopanel was manufactured by Dean Products, Inc., and consists of two 12 inch by 20 inch type 304 stainless steel sheets welded at the edges. One side is embossed and the panel is electro-polished. A drawing is shown in Figure 17.

(d) Vacuum Pumping System.

A six inch, four stage, fractionating diffusion pump capable of pumping 1500 liters/sec and with a blank off pressure of 10^{-7} torr was used to pump down the chamber. Dow Corning 704 fluid was used. This pump was backed by an NRC 100 CFM, single stage

mechanical pump with a blank off pressure of 10 to 15 microns. A liquid nitrogen trap was installed above the diffusion pump with an automatic fill system.

(e) Instrumentation.

Pressure measurements were made with Vacuum Electronics Corporation thermocouple gages down to 10^{-3} torr, and with Bayard-Alpert ionization gages and a General Electric cold cathode trigger gage below 10^{-3} torr. The G. E. gage and one glass envelope Bayard-Alpert gage was installed in the chamber wall, while a nude Bayard-Alpert gage was installed within the shielded volume.

Temperature measurements were made with teflon-insulated, 24 gage copper-constantan thermocouples installed on the cryopanel and shields. A schematic of the thermocouple locations is shown in Figure 5. A National Bureau of Standards computer program was used to calibrate the thermocouples (16). The thermocouple output was connected to a differential amplifier, then to a digital volt-meter with automatic printer for convenience.

All electrical controls are located in a desk top panel as shown in Figure 15. The system is arranged so that a high chamber pressure or a power failure will secure power to the diffusion pump and isolate the chamber by shutting the high vacuum and foreline valves. Power to the diffusion pump is also secured in the event of high diffusion pump temperatures.

APPENDIX B

Cryogenic Fluid Transfer System

A schematic of the cryogenic fluid transfer system is shown in Figure 18. The cold helium gas is transferred to the cryopanel through vacuum jacketed transfer lines designed and built by Tedeschi (18). The helium refrigerator was manufactured by A. D. Little.

Liquid nitrogen is transferred to the radiation shields and diffusion pump trap through 3/8 inch nylon lines insulated with 3/4 inch thick foam rubber Armaflex tubing. A manifold with Jamesbury cryogenic valves provides for separate filling and flow rate control to each shield section and the diffusion pump trap. A 172 liter dewar flask pressurized with 8 psig helium was used to supply liquid nitrogen to the transfer system.

APPENDIX C

Gas Addition and Flow Measurement System

The system used for controlling and measuring the flow of test gas is shown schematically in Figure 6. An indirect method was used in order to measure the flow rate with the required accuracy. The procedure was to evacuate a known volume and measure the rate of pressure rise in that volume. A variable leak valve was used to set the flow rate at an approximate value indicated on the counter. The pressure rise was recorded from a thermocouple gage and the flow rate then calculated from

$$Q_L = \dot{P} V \qquad (C.1)$$

In each case a background leakage pressure rise was determined and subtracted from $\dot{P}$.

The system was arranged as follows to measure the flow rate.

(a) Valves #2 and #3 are shut.

(b) Valve #1 is opened and the variable leak valve set to any desired value.

(c) The high vacuum valve for the auxiliary system is shut, and the rate of pressure rise in the auxiliary volume is measured.

(d) The flow of gas is secured with the gas isolation valve and the auxiliary volume and associated piping are pumped down with the auxiliary pumping system. The variable leak valve must be kept at the value set in (b) above.

(e) Valve #1 is then shut and valve #3 opened. The gas flow is re-established by opening the gas isolation valve and flow is now directed to the main vacuum chamber.

APPENDIX D

Operating Procedures

I. Vacuum System (Figure 2)

A. Initial pumpdown from atmospheric pressure.

1. Check the oil level in the bearing lubricating caps and the pumping chamber of the forepump. Turn on the forepump cooling water. The water is thermostatically controlled at the pump and will not flow unless the pump temperature reaches 180°F.

2. Close disconnect and breakers for forepump, solenoids, and diffusion pump.

3. Open valves for air supply to solenoid valves. Insure air pressure of 90 psig is available.

4. Check that all vent valves, doors and ports are shut.

5. Place overpressure switch on "Out".

6. Energize the solenoids and open the high vacuum valve and the foreline valve. Open the roughing valve manually.

7. Insure quick acting gas addition valve is shut. (Figure 6).

8. Start the forepump and monitor chamber pressure on chamber thermocouple pressure gage.

9. Turn on cooling water to the diffusion pump and cold cap. Insure quick cool valve is shut.

10. When pressure in the tank reaches 70 microns, energize the diffusion pump heaters. The pump requires about 20 minutes to become operational. Monitor the foreline pressure with the foreline thermocouple pressure gage. Initiation of pumping is indicated by a temporary rise in foreline pressure and a rapid decrease in chamber pressure.

11. When the diffusion pump is in operation, shut the roughing valve to prevent backstreaming of forepump oil into the chamber.

12. When the pressure is below 1 micron, energize the ionization gage and monitor tank pressure. Operation is outlined in the manual for the gage controller.

13. When pressure is below 10^{-4} torr, fill the diffusion pump cryogenic trap to reduce backstreaming of diffusion pump oil.

14. When leaving system unattended, place overpressure protection switch on "In".

B. To open the chamber.

1. Shut the high vacuum valve.

2. Open the chamber vent valve.

3. Keep the forepump and diffusion pump operating.

4. When the pressure is equalized, open the chamber.

C. To re-evacuate the chamber.

1. Shut the chamber vent valve.

2. Shut the foreline valve.

3. Open the roughing valve.

4. When the chamber pressure is less than 70 microns, shut the roughing valve, open the foreline valve, open the high vacuum valve.

If the chamber is to be open for only a short period of time, the use of dry nitrogen gas to bring the chamber to atmospheric pressure will considerably reduce the subsequent pumpdown time.

D. To shut the system down completely.

1. Shut the high vacuum valve.

2. De-energize the diffusion pump heaters and turn on the quick cool water.

3. When the diffusion pump is cool, shut the foreline valve and secure the forepump.

4. Open the chamber vent valve and the foreline vent valve to equalize the pressure and then shut these valves.

5. Secure all cooling water.

6. Secure all electrical power.

II. Cryogenic Transfer System.

A. Liquid nitrogen transfer.

1. Connect liquid nitrogen dewar to cryogenic line with rubber tubing.

2. Pressurize dewar to 8 psig with helium.

3. Energize diffusion pump trap automatic level control valve.

4. Insure Armaflex connection fits tightly around supply lines to shields.

5. Open transfer valves and observe exhaust.

6. Monitor thermocouples to check liquid level in the shields.

7. When shields are approximately half full, reduce flow by partially shutting transfer valves. This will help to prevent geysering from the vent lines.

8. It will be necessary to maintain flow to the shields to replace evaporation losses and maintain uniform temperatures.

B. Helium transfer.

1. Pump vacuum jackets on transfer lines to approximately 15 microns.

2. Start and cool down helium refrigerator.

3. When refrigerator is cool, start the gas transfer.

4. Monitor panel temperature with thermocouples.

III. Flow measurement system (Figure 6).

1. Open valves #1, #2, quick-acting valve and auxiliary system high vacuum valve.

2. Shut valve #3 and the variable leak valve.

3. Open the gas isolation valve.

4. With auxiliary pumping system pumping on the auxiliary volume, use the variable leak valve to set the desired pressure in the auxiliary volume.

To measure flow by measuring the rate of pressure rise in the auxiliary volume.

1. Insure gas isolation valve and quick-acting valve are shut.

2. Open valves #1, #2, #3. Open the variable leak valve to the fully open position.

3. Pump down with the auxiliary pumping system.

4. Shut valves #2 and #3.

5. Set variable leak valve to desired setting.

6. Shut auxiliary system high vacuum valve.

7. Open the gas isolation valve and record P versus t.

8. Shut gas isolation valve, open auxiliary system high vacuum valve and pump auxiliary system down as far as possible.

9. Shut valve #1, open valve #3 and the quick-acting valve.

10. Open the gas isolation valve.

APPENDIX E

Model Analysis of ΔP

In order to ensure that the measured pressure drop is in fact the pressure drop derived in equation (4.1), a model was proposed and analyzed by Tedeschi in 1966, and improved by Bevan in 1967 (18,3). The complete analysis is included here since it is deemed so important to the experimental method of determining capture coefficients.

The system consists of a chamber in which is mounted a cylindrical radiation shield, two circular disk end shields and a gas addition system. The actual system is described in Appendix A. The model as shown in Figure 19 consists of three volumes. The chamber is divided into an inner volume V_i and an outer volume V_o by the radiation shielding. Conductance between the two volumes consists of two circular viewing ports in the end shields and a clearance between the end shields and the cylindrical shield. The gas addition volume V_a consists of tubing leading the gas from the controlled leak supply to the inner volume. Referring to Figure 19, the volumes, temperatures and molecular flow rates that must be considered are:

V_a - Volume of piping between gas injection stop valve and chamber

V_i - Volume of the chamber inside the radiation shielding

V_o - Volume between the shielding and the tank wall

T_o - Mean temperature of tank wall and the radiation shielding

T_a - Temperature of the wall of the piping containing V_a

T_i - Temperature of the gas in V_i

T_L - Temperature of the gas admitted to V_a

$\dot{N}_L$ - Molecules/sec of controlled gas entering lines to the chamber

$\dot{N}_{ai}$ - Molecules/sec of controlled gas entering the inner volume V_i from V_a

$\dot{N}_c$ - Molecules/sec of condensable gas captured by the cryosurface

$\dot{N}_{io}$ - Molecules/sec of gas entering the outer volume V_o from V_i

$\dot{N}_D$ - Molecules/sec of condensable gas pumped by the diffusion pump and the cryogenic trap

$\dot{N}_{ra}$, $\dot{N}_{ri}$, $\dot{N}_{ro}$ - Molecules/sec of residual condensable gas from leakage into the chamber and outgassing of materials within the chamber

$\dot{N}_i$ - Summation of all gas fluxes into V_i

$\dot{N}_o$ - Summation of all gas fluxes into V_o

$\dot{N}_a$ - Summation of all gas fluxes into V_a

Expression for each of the molecular flow rates are developed in terms of measurable quantities as follows:

(1) $\dot{N}_i$, $\dot{N}_o$, $\dot{N}_a$

From the ideal gas law

$$N = \frac{PVN_A}{RT}$$

$$\dot{N} = \frac{1}{k} \frac{d}{dt} \left[\frac{PV}{T} \right]$$

The gases all occupy the same constant volumes. As will be seen later, the temperature in any given volume must be assumed constant.

Therefore,

$$\dot{N} = \frac{V}{kT}\dot{P}$$

and

$$\dot{N}_i = \frac{V_i}{kT_i}\dot{P}_i \qquad \text{(E.1)}$$

$$\dot{N}_o = \frac{V_o}{kT_o}\dot{P}_o \qquad \text{(E.2)}$$

$$\dot{N}_a = \frac{V_a}{kT_a}\dot{P}_a \qquad \text{(E.3)}$$

(2) $\dot{N}_L$

The flow of controlled gas is

$$\dot{N}_L = \frac{1}{k}\frac{d}{dt}\left[\frac{P_L V_L}{T_L}\right]$$

where P_L and T_L are the pressure and temperature at the inlet to the gas addition piping and are constant so that

$$\dot{N}_L = \frac{P_L \dot{V}_L}{kT_L} = \frac{Q_L}{T_L} \qquad \text{(E.4)}$$

(3) $\dot{N}_{ai}$, $\dot{N}_{io}$

From kinetic theory, the number of molecules incident on a surface per unit time is

$$\dot{N} = \frac{PA}{(2\pi m k T)^{1/2}} \qquad (3.7)$$

Then

$$\dot{N}_{ai} = C_a\left[\frac{P_a}{\sqrt{T_a}} - \frac{P_i}{\sqrt{T_i}}\right] \qquad \text{(E.5)}$$

where

$$C_a = \frac{A_{ai}}{(2\pi m k)^{1/2}}$$

and A_{ai} is the area through which the gas flows as it travels from V_a to V_i. Similarly,

$$\dot{N}_{io} = C_i \left[\frac{P_i}{\sqrt{T_i}} - \frac{P_o}{\sqrt{T_o}} \right] \qquad \text{(E.6)}$$

(4) $\dot{N}_c$

The expression for the flow to the cryopanel is given by equation (3.24).

$$\dot{N}_c = \frac{A_s}{(2\pi m k)^{1/2}} \left[\frac{f_g P_i}{\sqrt{T_i}} - \frac{f_s P_s}{\sqrt{T_s}} \right] \qquad \text{(3.24)}$$

(5) $\dot{N}_D$

The volumetric pumping speed of a diffusion pump can be considered constant over the pressure range of interest here. The pumping speed curve for the pump employed in this system is shown in Figure 20. Since pressure change has no effect on the pumping speed,

$$\dot{N}_D = \frac{P}{kT} \dot{V}_D \qquad \text{(E.7)}$$

If, as in this system, the diffusion pump is used with a cryogenic trap, the limited conductance of the trap will reduce $\dot{V}_D$ and

$$\dot{N}_D = \left[\frac{\alpha \dot{V}_D}{k T_o} \right] P_o \qquad \text{(E.8)}$$

where α is an efficiency factor.

(6) $\dot{N}_r$

After exposure to atmospheric air for several hours, the amount of gas readily available for desorption from a surface at room temperature amounts to many molecular layers. Although the outgassing rate of a material is time dependent, after exposure to vacuum for considerable periods, the variation with time is small. For example, Dayton (10) shows that after ten hours of vacuum pumping, the outgassing rate for a stainless steel surface is 1×10^{-8} torr liter/sec-cm^2 and is decreasing very slowly. Since the time required for measurements is small, the outgassing rate will be considered constant.

$$\dot{N}_r = \frac{1}{k} \frac{d}{dt}\left[\frac{PV}{T}\right] = \frac{Q_r}{kT} \qquad \text{(E.9)}$$

where Q_r is the outgassing rate from a given surface.

The diffusion of a gas through metal is proportional to the square root of the pressure. The rate of diffusion is small and the pressure changes in the system are very small. The leakage rate is therefore considered constant and will be included in the term for outgassing. Measurements of the combined effects of outgassing and leakage in this system at room temperature indicated that these effects were constant over the short periods of time required for measurements. Therefore,

$$\dot{N}_{ra} = \frac{Q_{ra}}{k T_a} \qquad \text{(E.10)}$$

$$\dot{N}_{ri} = \frac{Q_{ri}}{k T_i} \qquad \text{(E.11)}$$

$$\dot{N}_{ro} = \frac{Q_{ro}}{k T_o} \tag{E.12}$$

The following equations result from molecular rate balances on the three volumes shown in Figure 19.

$$\dot{N}_i = \dot{N}_{ri} + \dot{N}_{ai} - \dot{N}_c - \dot{N}_{io} \tag{E.13}$$

$$\dot{N}_o = \dot{N}_{io} + \dot{N}_{ro} - \dot{N}_D \tag{E.14}$$

$$\dot{N}_a = \dot{N}_L + \dot{N}_{ra} - \dot{N}_{ai} \tag{E.15}$$

Substitution of the expressions developed for the terms in these equations and solution for the rate of pressure change in each volume yields

$$\dot{P}_i = \frac{Q_{ri}}{V_i} + \left[\frac{f_s A_s T_i}{V_i}\left(\frac{k}{2\pi m T_s}\right)^{\frac{1}{2}}\right] P_s + \left[\frac{C_i k T_i}{V_i \sqrt{T_o}}\right] P_o \tag{E.16}$$

$$+ \left[\frac{C_a k T_i}{V_i \sqrt{T_a}}\right] P_a - \left[\frac{C_o k T_i^{\frac{1}{2}}}{V_i} + \frac{f_g A_s}{V_i}\left(\frac{k T_i}{2\pi m}\right)^{\frac{1}{2}} + \frac{C_i k T_i^{\frac{1}{2}}}{V_i}\right] P_i$$

$$\dot{P}_o = \frac{Q_{ro}}{V_o} + \left[\frac{C_i k T_o}{V_o T_i^{1/2}}\right] P_i - \left[\frac{\alpha \dot{V}_o}{V_o} + \frac{C_i k T_o^{\frac{1}{2}}}{V_o}\right] P_o \tag{E.17}$$

$$\dot{P}_a = \frac{Q_{ra}}{V_a} + \frac{Q_L T_a}{V_a T_i} + \left[\frac{C_a k T_a}{V_a T_i^{1/2}}\right] P_i - \left[\frac{C_a k T_a^{1/2}}{V_a}\right] P_a \tag{E.18}$$

By defining constants as in Table XIII, the equations above can be expressed as

$$\dot{P}_i = A + a_1 P_o + a_2 P_a - \left[a_3 + a_4 + a_5\right] P_i \qquad \text{(E.19)}$$

$$\dot{P}_o = B + a_6 P_i - \left[a_7 + a_8\right] P_o \qquad \text{(E.20)}$$

$$\dot{P}_a = C + D + a_9 P_i - a_{10} P_a \qquad \text{(E.21)}$$

These are the equations which describe the system. They have been solved on an analog computer by Tedeschi (18), and curves similar to that shown in Figure 3 have been obtained. Reference to Figure 3 and to equations (E.19), (E.20) and (E.21) yield the following solutions for steady state operations between times t_1 and t_2.

$$P_i(I) = \frac{a_{10}(a_7+a_8)A + a_1 a_{10} B + a_2(a_7+a_8)(C+D)}{a_{10}(a_7+a_8)(a_3+a_4+a_5) - a_1 a_6 a_{10} - a_2 a_9 (a_7+a_8)} \qquad \text{(E.22)}$$

$$P_o(I) = \frac{B}{a_7 + a_8} + \frac{a_6}{a_7 + a_8} P_i(I) \qquad \text{(E.23)}$$

$$P_a(I) = \frac{C + D}{a_{10}} + \frac{a_9}{a_{10}} P_i(I) \qquad \text{(E.24)}$$

At time t_2, the diffusion pump is isolated from the system and therefore, $a_7 = \propto \dot{V}_D/V_o = 0$, and the equilibrium solutions are:

$$P_i(II) = \frac{a_{10}a_8A + a_1a_{10}B + a_2a_8(C+D)}{a_{10}a_8(a_3 + a_4 + a_5) - a_1a_6a_{10} - a_2a_8a_9} \qquad \text{(E.25)}$$

$$P_o(II) = \frac{B}{a_8} + \frac{a_6}{a_8} P_i(II) \qquad \text{(E.26)}$$

$$P_a(II) = \frac{C + D}{a_{10}} + \frac{a_9}{a_{10}} P_i(II) \qquad \text{(E.27)}$$

At time t_3, the gas inflow is abruptly halted and therefore, $D = Q_L T_a / V_L T_L = 0$. The equilibrium solutions are:

$$P_i(III) = \frac{a_{10}a_8A + a_1a_{10}B + a_2a_8C}{a_{10}a_8(a_3 + a_4 + a_5) - a_1a_6a_{10} - a_2a_8a_9} \qquad \text{(E.28)}$$

$$P_o(\text{III}) = \frac{B}{a_8} + \frac{a_6}{a_8} P_i(\text{III}) \qquad \text{(E.29)}$$

$$P_a(\text{III}) = \frac{C}{a_{10}} + \frac{a_9}{a_{10}} P_i(\text{III}) \qquad \text{(E.30)}$$

The pressure drop in the inner volume is then

$$P_i(\text{II}) - P_i(\text{III}) = \frac{a_2 a_8 D}{a_8 a_{10}(a_3 + a_4 + a_5) - a_1 a_6 a_{10} - a_2 a_8 a_9} \qquad \text{(E.31)}$$

and substitution of the constants from Table XIII yields

$$P_i(\text{II}) - P_i(\text{III}) = \frac{Q_L T_i}{f_g A_s T_L} \left[\frac{2\pi M}{R T_i}\right]^{\frac{1}{2}} \frac{T_i}{T_L}$$

or

$$f_g = \frac{Q_L}{A_s \left[P_i(\text{II}) - P_i(\text{III})\right]} \left[\frac{2\pi M}{R T_i}\right]^{\frac{1}{2}} \frac{T_i}{T_L} \qquad \text{(E.32)}$$

This is the same expression as equation (4.1) when it is considered that:

T_i is the temperature of the gas in the inner volume and is therefore equal to T_g.

P_i (II) is the equilibrium pressure with gas flow being admitted to the chamber and is therefore equal to P_e.

P_i(III) is the equilibrium pressure with no gas flow to the chamber and is therefore equal to P_g.

$$\Delta P = P_i(II) - P_i(III) = P_e - P_g$$

The experimentally observed pressure drop is therefore the same as that predicted by the theory providing the assumptions mentioned previously are valid and provided that the experimental pressure drop is measured in the inner volume V_i.

If the experimental pressure is measured in V_o, then the equations for the system predict

$$P_o(II) - P_o(III) = \frac{a_6}{a_8}\left[P_i(II) - P_i(III)\right] \qquad (E.33)$$

Substitution of the constants results in

$$P_o(II) - P_o(III) = \sqrt{\frac{T_o}{T_i}}\left[P_i(II) - P_i(III)\right] \qquad (E.34)$$

which indicates that an application of the thermal transpiration effect is all that is required to relate the pressure drop measured in the outer volume to the pressure drop measured in the inner volume. The measurement of the pressure drop in the outer volume however, may not accurately reflect the rate of incidence of molecules on the cryosurface. If the conductance between the inner and outer volumes is not large, this conductance may have a significant effect on the measurement of the capture coefficient.

If the two volumes are considered connected by a conductance of area β, with the gas inflow into V_i as shown in Figure 21, the effect of the conductance may be determined in the following manner.

At steady state,

$$\frac{N_A P_L \dot{V}_L}{R T_L} = \frac{f A P_i}{(2\pi m k T_i)^{1/2}} \qquad \text{(E.35)}$$

and

$$\frac{\beta P_o}{(2\pi m k T_o)^{1/2}} - \frac{\beta P_i}{(2\pi m k T_i)^{1/2}} = \frac{f A P_i}{(2\pi m k T_i)^{1/2}} \qquad \text{(E.36)}$$

Solution of both equations for P_i and a subtraction yields,

$$P_o - \frac{N_A P_L \dot{V}_L}{\beta R T_L}(2\pi m k T_o)^{1/2} = \frac{N_A P_L \dot{V}_L}{A f R T_L}(2\pi m k T_o)^{1/2} \qquad \text{(E.37)}$$

P_o can be eliminated by using thermal transpiration and if $T_m = T_L$, then

$$P_m S_{TH} - \frac{P_L \dot{V}_L}{\beta} = \frac{P_L \dot{V}_L}{A f} \qquad \text{(E.38)}$$

and solving for the capture coefficient

$$f = \frac{\beta Q_L}{\beta A P_m S_{TH} - A P_L \dot{V}_L} \qquad \text{(E.39)}$$

If f* is the capture coefficient measured without any conductance effects, then equation (3.18) can be expressed as

$$f^* = \frac{Q_L}{A S_{TH} P_m} \qquad \text{(E.40)}$$

The ratio of these two capture coefficients is

$$\frac{f^*}{f} = \frac{\beta - f^* A}{\beta} \qquad \text{(E.41)}$$

so that unless the product of the cryosurface area and the capture coefficient without conductance (f*) is small compared to the conductance area, the effect cannot be ignored. In order to eliminate the effect of limited conductance, it is desirable to measure the pressure in the volume containing the cryosurface.

APPENDIX F

Sample Data Reduction

1. Flow rate, Q_L, was determined from equation (C.1)

$$Q = \dot{P} V$$

where V = 4.35 liters

2. The condensation coefficient f_g was determined from equation (4.2)

$$f_g = \frac{Q_L T_g}{A_s T_L \Delta P (G.F.)} \left[\frac{2\pi M}{R T_g}\right]^{\frac{1}{2}}$$

Rearranging terms and substituting in system constants yields

$$f_g = 8.35 \times 10^{-5} \left[\frac{Q_L}{\Delta P (G.F.)}\right] \frac{\sqrt{T_g M}}{T_L}$$

where required units are:

Q_L in torr liter/sec

ΔP in torr

Temperature in °K

Gage factors are:

1.00 for nitrogen

0.73 for carbon dioxide

0.84 for argon

3. The condensation coefficient corrected for conductance was determined from equation (4.4)

$$f_g^* = \frac{1}{\frac{1}{f_g} + 0.425}$$

where β = 7780 cm^2

4. Sample calculation from the high flow rate carbon dioxide experiment. (Figure 9, Table III).

$\dot{P}$ = 50.4 μ/sec

$V = 4.35$ liter

$T_g = 293.5°K$

$M = 44$

$T_L = 294.8°K$

$\Delta P = 20.343 \times 10^{-6}$ torr

G.F. = 0.73

$t = 65.4$ sec $= 1.09$ min

$T_s = 24°K$

$$Q_L = \dot{P} V$$

$$= \left(50.4 \frac{\mu}{sec}\right)\left(\frac{1 \text{ torr}}{10^3 \mu}\right)(4.35 \text{ Liter}) = 0.219 \text{ torr Liter/sec}$$

$$f_g = 8.35 \times 10^{-5} \left[\frac{Q_L}{\Delta P \,(G.F.)}\right] \frac{\sqrt{T_g M}}{T_L}$$

$$= 8.35 \times 10^{-5} \left[\frac{0.219 \text{ torr Liter/sec}}{(20.343 \times 10^{-6} \text{ torr})(0.73)}\right] \frac{\sqrt{(293.5°K)(44)}}{294.8°K} = 0.474$$

$$f_g^* = \frac{1}{\frac{1}{f_g} + 0.425} = \frac{1}{\frac{1}{0.474} + 0.425} = 0.395$$

APPENDIX G

Computer Program for Data Reduction

```
      THIS PROGRAM CALCULATES THE CAPTURE COEFFICIENT CORRECTED
      FOR CONDUCTANCE EFFECTS

      IMPLICIT REAL*8(A-H),REAL*8(O-Z)
      DIMENSION TIME(100),FG(100),FSTAR(100),TG(100),
     1TL(100),DELTAP(100)

      READ THE FOLLOWING INPUTS
            NO=NUMBER OF DATA POINTS IN EXPERIMENT
            Q=FLOW RATE IN TORR LITER/SEC
            FORM=FORMULA WEIGHT
            GF=GAGE FACTOR

   10 READ (5,11) NO,Q,FORM,GF
   11 FORMAT (I110,3F10.0)
      IF (NO-2) 101, 100, 101
  101 CONTINUE
      DO 13 I=1,NO

      READ THE FOLLOWING INPUTS
            DELTAP=PRESSURE DROP IN TORR TIMES 10 +6 POWER
            TIME=TIME IN SECONDS
            TG=GAS TEMPERATURE IN DEGREES K
            TL=LEAK TEMPERATURE IN DEGREES K

      READ (5,12)DELTAP(I),TIME(I),TG(I),TL(I)
   12 FORMAT(4F10.0)
   13 CONTINUE
      WRITE (6,14)
   14 FORMAT (1H1)
  600 WRITE (6,601)
  601 FORMAT(/,/,10X,9HFLOW RATE,/)
  602 WRITE(6,603) Q
  603 FORMAT(10X,F9.7)
  604 WRITE(6,605)
  605 FORMAT(/,/,12X,5HCAPCO,18X,4HTIME,/)
  606 DO 611 I=1,NO
  650 DELTAP(I)=DELTAP(I)*1.D-6
  651 TIME(I)=TIME(I)/60.

      CALCULATE CAPTURE COEFFICIENT MEASURED WITH CONDUCTANCE

  607 FG(I)=(8.350-5)*(Q/(DELTAP(I)*GF))*((DSQRT(TG(I)
     1*FORM))/TL(I))

      CALCULATE CAPTURE COEFFICIENT MEASURED WITHOUT CONDUCTANCE

  608 FSTAR(I)=1./((1./FG(I))+0.425)

  609 WRITE (6,610) FSTAR(I),TIME(I)
  610 FORMAT (10X,F10.8,10X,F10.5)
  611 CONTINUE
      GO TO 10
  100 CONTINUE
      END
```

```
FIRST DATA CARD
        16.219          44.             .73

SECOND DATA CARD
20.343      65.4        293.5       294.8

ADD A DATA CARD FOR EACH POINT TO BE DETERMINED

LAST DATA CARD MUST CONTAIN THESE NUMBERS
          21.           1.              1.
```

INITIAL DISTRIBUTION LIST

		No. Copies
1.	Defense Documentation Center Cameron Station Alexandria, Virginia 22314	20
2.	Library Naval Postgraduate School Monterey, California 93940	2
3.	Naval Ship Systems Command Navy Department Washington, D. C. 20360	1
4.	Mechanical Engineering Department Naval Postgraduate School Monterey, Calif. 93940	1
5.	Prof. Paul F. Pucci Mechanical Engineering Department Naval Postgraduate School Monterey, Calif. 93940	5
6.	LCDR Vernon R. Everly, USN San Francisco Bay Naval Shipyard Mare Island Vallejo, Calif. 94592	2
7.	LCDR J. A. Bevan, USN Norfolk Naval Shipyard Portsmouth, Virginia 23709	1
8.	LT L. C. Tedeschi, USN Supervisor of Shipbuilding, U. S. Navy Bath Iron Works Bath, Maine 04530	1
9.	LCDR Carl Albero , USN Supervisor of Shipbuilding, U. S. Navy Bath Iron Works Bath, Maine 04530	1
10.	LCDR G. M. LaChance Naval Ship Systems Command Code 1500 Navy Department Washington, D. C. 20360	1

DOCUMENT CONTROL DATA - R&D

(Security classification of title, body of abstract and indexing annotation must be entered when the overall report is classified)

1. ORIGINATING ACTIVITY (Corporate author)

Naval Postgraduate School
Monterey, California 93940

2a. REPORT SECURITY CLASSIFICATION

Unclassified

2b. GROUP

3. REPORT TITLE

The Bare Surface Effect in Cryogenic Pumping

4. DESCRIPTIVE NOTES (Type of report and inclusive dates)

5. AUTHOR(S) (Last name, first name, initial)

EVERLY, Vernon Richard

6. REPORT DATE	7a. TOTAL NO. OF PAGES	7b. NO. OF REFS
September 1967	96	20

8a. CONTRACT OR GRANT NO.	9a. ORIGINATOR'S REPORT NUMBER(S)
b. PROJECT NO. N/A	N/A
c.	9b. OTHER REPORT NO(S) (Any other numbers that may be assigned this report) N/A
d.	

10. AVAILABILITY/LIMITATION NOTICES

This document is subject to special export controls and each transmittal to foreign nationals may be made only with prior approval of the Naval Postgraduate School.

11. SUPPLEMENTARY NOTES	12. SPONSORING MILITARY ACTIVITY

13. ABSTRACT

Capture coefficients were measured for nitrogen, carbon dioxide and argon as a function of gas flow time in order to determine whether a bare surface effect existed. The effect was observed only with 300°K nitrogen on a 20°K and 24°K cryopanel and with 300°K carbon dioxide on an 82°K cryopanel. Cryopanel temperature was determined to be the only parameter influencing the bare surface effect. Capture coefficient values were representative of those reported in the literature and their dependence upon flow rate was confirmed.

14. KEY WORDS	LINK A		LINK B		LINK C	
	ROLE	WT	ROLE	WT	ROLE	WT
Bare surface effect						
Cryogenic Pumping						
High Vacuum						
Capture Coefficient						

INSTRUCTIONS

1. ORIGINATING ACTIVITY: Enter the name and address of the contractor, subcontractor, grantee, Department of Defense activity or other organization *(corporate author)* issuing the report.

2*a*. REPORT SECURITY CLASSIFICATION: Enter the overall security classification of the report. Indicate whether "Restricted Data" is included. Marking is to be in accordance with appropriate security regulations.

2*b*. GROUP: Automatic downgrading is specified in DoD Directive 5200.10 and Armed Forces Industrial Manual. Enter the group number. Also, when applicable, show that optional markings have been used for Group 3 and Group 4 as authorized.

3. REPORT TITLE: Enter the complete report title in all capital letters. Titles in all cases should be unclassified. If a meaningful title cannot be selected without classification, show title classification in all capitals in parenthesis immediately following the title.

4. DESCRIPTIVE NOTES: If appropriate, enter the type of report, e.g., interim, progress, summary, annual, or final. Give the inclusive dates when a specific reporting period is covered.

5. AUTHOR(S): Enter the name(s) of author(s) as shown on or in the report. Enter last name, first name, middle initial. If military, show rank and branch of service. The name of the principal author is an absolute minimum requirement.

6. REPORT DATE: Enter the date of the report as day, month, year; or month, year. If more than one date appears on the report, use date of publication.

7*a*. TOTAL NUMBER OF PAGES: The total page count should follow normal pagination procedures, i.e., enter the number of pages containing information.

7*b*. NUMBER OF REFERENCES: Enter the total number of references cited in the report.

8*a*. CONTRACT OR GRANT NUMBER: If appropriate, enter the applicable number of the contract or grant under which the report was written.

8*b*, 8*c*, & 8*d*. PROJECT NUMBER: Enter the appropriate military department identification, such as project number, subproject number, system numbers, task number, etc.

9*a*. ORIGINATOR'S REPORT NUMBER(S): Enter the official report number by which the document will be identified and controlled by the originating activity. This number must be unique to this report.

9*b*. OTHER REPORT NUMBER(S): If the report has been assigned any other report numbers *(either by the originator or by the sponsor)*, also enter this number(s).

10. AVAILABILITY/LIMITATION NOTICES: Enter any limitations on further dissemination of the report, other than those imposed by security classification, using standard statements such as:

(1) "Qualified requesters may obtain copies of this report from DDC."

(2) "Foreign announcement and dissemination of this report by DDC is not authorized."

(3) "U. S. Government agencies may obtain copies of this report directly from DDC. Other qualified DDC users shall request through _____."

(4) "U. S. military agencies may obtain copies of this report directly from DDC. Other qualified users shall request through _____."

(5) "All distribution of this report is controlled. Qualified DDC users shall request through _____."

If the report has been furnished to the Office of Technical Services, Department of Commerce, for sale to the public, indicate this fact and enter the price, if known.

11. SUPPLEMENTARY NOTES: Use for additional explanatory notes.

12. SPONSORING MILITARY ACTIVITY: Enter the name of the departmental project office or laboratory sponsoring *(paying for)* the research and development. Include address.

13. ABSTRACT: Enter an abstract giving a brief and factual summary of the document indicative of the report, even though it may also appear elsewhere in the body of the technical report. If additional space is required, a continuation sheet shall be attached.

It is highly desirable that the abstract of classified reports be unclassified. Each paragraph of the abstract shall end with an indication of the military security classification of the information in the paragraph, represented as *(TS)*, *(S)*, *(C)*, or *(U)*.

There is no limitation on the length of the abstract. However, the suggested length is from 150 to 225 words.

14. KEY WORDS: Key words are technically meaningful terms or short phrases that characterize a report and may be used as index entries for cataloging the report. Key words must be selected so that no security classification is required. Identifiers, such as equipment model designation, trade name, military project code name, geographic location, may be used as key words but will be followed by an indication of technical context. The assignment of links, roles, and weights is optional.